EC Journals.ASM.org

Host Erythrocyte Environment Influences the Localization of Exported Protein 2, an Essential Component of the *Plasmodium* Translocon

Elamaran Meibalan, Mary Ann Comunale, Ana M. Lopez, Lawrence W. Bergman, Anand Mehta, Akhil B. Vaidya, James M. Burns, Jr.

Center for Molecular Parasitology, Department of Microbiology and Immunology, Drexel University, Philadelphia, Pennsylvania, USA

Malaria parasites replicating inside red blood cells (RBCs) export a large subset of proteins into the erythrocyte cytoplasm to facilitate parasite growth and survival. PTEX, the parasite-encoded translocon, mediates protein transport across the parasitophorous vacuolar membrane (PVM) in *Plasmodium falciparum*-infected erythrocytes. Proteins exported into the erythrocyte cytoplasm have been localized to membranous structures, such as Maurer's clefts, small vesicles, and a tubovesicular network. Comparable studies of protein trafficking in *Plasmodium vivax*-infected reticulocytes are limited. With *Plasmodium yoelii*-infected reticulocytes, we identified exported protein 2 (Exp2) in a proteomic screen of proteins putatively transported across the PVM. Immunofluorescence studies showed that *P. yoelii* Exp2 (*Py*Exp2) was primarily localized to the PVM. Unexpectedly, *Py*Exp2 was also associated with distinct, membrane-bound vesicles in the reticulocyte cytoplasm. This is in contrast to *P. falciparum* in mature RBCs, where *P. falciparum* Exp2 (*Pf*Exp2) is exclusively localized to the PVM. Two *P. yoelii*-exported proteins, PY04481 (encoded by a *pyst-a* gene) and PY06203 (*Py*pAg-1), partially colocalized with these *Py*Exp2-positive vesicles. Further analysis revealed that with *P. yoelii*, *Plasmodium berghei*, and *P. falciparum*, cytoplasmic Exp2-positive vesicles were primarily observed in CD71$^+$ reticulocytes versus mature RBCs. In transgenic *P. yoelii* 17X parasites, the association of hemagglutinin-tagged *Py*Exp2 with the PVM and cytoplasmic vesicles was retained, but the *pyexp2* gene was refractory to deletion. These data suggest that the localization of Exp2 in mouse and human RBCs can be influenced by the host cell environment. Exp2 may function at multiple points in the pathway by which parasites traffic proteins into and through the reticulocyte cytoplasm.

An estimated 3.4 billion people in 103 countries live in areas of malaria transmission, with populations living in sub-Saharan Africa having the highest risk of acquiring the disease (1). In 2012, the World Health Organization reported 207 million cases with an estimated 473,000 to 789,000 deaths worldwide, most due to *Plasmodium falciparum* infections in young children. The severity of *P. falciparum* malaria is attributed to the high parasite burden and the sequestration of mature parasitized red blood cells (RBCs) in the microvasculature (2). *P. falciparum* malaria predominates in Africa, but *Plasmodium vivax* infections are more widely distributed (3). *P. vivax* malaria is less often fatal, in part because the parasite preferentially invades reticulocytes, which are limited in peripheral circulation (0.5 to 1.5% of the total red blood cells in adults) (4). However, the increased recognition of severe clinical syndromes associated with *P. vivax* is a growing concern (5).

Mammalian *Plasmodium* spp. invade erythrocytes, which are generally devoid of cellular organelles and components of protein synthesis/trafficking machinery. The parasite replicates within a parasitophorous vacuolar membrane (PVM) but remodels the host cell, altering its permeability, metabolism, and adhesive characteristics (6–8). To do this, parasite proteins are exported across the PVM into the host cytoplasm and trafficked to the RBC surface for nutrient import and cytoadherence (9, 10). The protein transport machinery includes parasite-derived membranous structures extending from the PVM that form a tubulovesicular network (TVN) (11) and disc-like structures in the RBC cytoplasm called Maurer's clefts (MCs) (12). A major virulence protein in *P. falciparum*, erythrocyte membrane protein 1 (*Pf*EMP1), is exported via MCs to the RBC surface (13), where it binds to vascular endothelial receptors (CD36, VCAM-1, ICAM-1, and CSA), promoting sequestration of infected red blood cells (iRBCs) (14–16). Other electron-dense vesicles (EDVs) with diameters of 60 to 100 nm (17, 18) and J-Dots (19) are also involved in the transport of parasite proteins through the RBC cytoplasm. These striking red cell modifications induced by *P. falciparum* are less well characterized in other plasmodial species.

In the prevailing model for export into the red cell cytoplasm, parasite proteins are secreted into the parasitophorous vacuole and then transported across the PVM. A conserved feature of several exported *P. falciparum* proteins is the presence of a pentameric recognition sequence (RxLxE/Q/D) called the PEXEL (*Plasmodium* export element) or HT (host-targeting) motif located ~25 amino acids downstream from the endoplasmic reticulum (ER) signal sequence (20, 21). Translocation of PEXEL-containing and PEXEL-negative exported proteins across the PVM is mediated by the same essential ATP-dependent, multimeric protein complex, called PTEX (*Plasmodium* translocon of exported proteins), located in the PVM (22–25). PTEX is comprised of five known components—heat shock protein HSP101, exported protein 2 (Exp2), thioredoxin 2 (TRX2), and two novel proteins, PTEX150 and PTEX88 (22, 26). The current model for PTEX function suggests that PEXEL/HT-containing proteins arrive at

Received 1 October 2014 **Accepted** 28 January 2015

Accepted manuscript posted online 6 February 2015

Citation Meibalan E, Comunale MA, Lopez AM, Bergman LW, Mehta A, Vaidya AB, Burns JM, Jr. 2015. Host erythrocyte environment influences the localization of exported protein 2, an essential component of the *Plasmodium* translocon. Eukaryot Cell 14:371–384. doi:10.1128/EC.00228-14.

Address correspondence to James M. Burns, Jr., jburns@drexelmed.edu.

Supplemental material for this article may be found at http://dx.doi.org/10.1128/EC.00228-14.

doi:10.1128/EC.00228-14

the PVM and are first unfolded, then inserted through a pore formed by multimers of Exp2, and finally refolded in the erythrocyte cytoplasm by parasite-encoded and/or host cell chaperones (22, 26, 27). Beyond the PVM, subsequent transport of exported proteins through the erythrocyte cytoplasm appears to involve distinct trafficking pathways and various membrane-bound structures and/or vesicles.

Studies of protein trafficking in reticulocyte-prone *P. vivax* have been limited due to the inability to grow blood-stage parasites in continuous culture and the low parasitemia associated with human infection. Comparative genome sequence analyses also did not reveal *P. falciparum* orthologues of Maurer's cleft-associated proteins present in *P. vivax* (28). Nevertheless, previous studies in *P. vivax* and *Plasmodium cynomolgi* (a closely related simian parasite) described elongated caveola-like structures complexed with 40- to 50-nm electron-dense vesicles in the cytoplasm of iRBCs (29, 30). The precise function of these structures in protein export was not clearly established. Recent studies of *Plasmodium berghei* in rodents identified dynamic tubular (31, 32) and vesicle-like (33) structures in the host cell cytoplasm potentially involved in parasite protein transport. These studies suggest that components of the protein export machinery may vary between *Plasmodium* spp. However, distinct host cell environments (reticulocytes, mature RBCs, and senescent RBCs) encountered by blood-stage parasites may also influence protein transport pathways in the RBC cytoplasm. This has not been explored. Given the presence of residual subcellular structures and RNA, reticulocytes present a unique environment for parasite growth in comparison to mature RBCs.

We began the present study to identify membrane-associated exported proteins in the reticulocyte-prone rodent parasite *Plasmodium yoelii* 17X. Our results indicate that Exp2, an integral component of the PVM-anchored PTEX, is also exported into the cytoplasm of *P. yoelii*-infected reticulocytes, associated with a subset of membrane-bound vesicles that contain additional parasite proteins. Importantly, Exp2-positive vesicles were preferentially observed in reticulocytes versus mature RBCs infected with *P. yoelii*, *P. berghei*, and *P. falciparum*. Our data suggest that the host cell type may influence the protein transport mechanisms used by blood-stage parasites and that in reticulocytes, Exp2 may function at multiple points in the export-transport pathway.

MATERIALS AND METHODS

Experimental animals and parasites. Five- to 6-week-old male BALB/cByJ mice were purchased from Jackson Laboratories (Bar Harbor, ME). All animals were housed in the animal care facility of Drexel University College of Medicine (Philadelphia, PA) under specific-pathogen-free conditions. Nonlethal *P. yoelii* 17X, lethal *P. yoelii* 17XL, and *P. berghei* ANKA parasites were originally obtained from William P. Weidanz (University of Wisconsin, Madison, WI) and maintained as cryopreserved stabilates. All animal studies were reviewed and approved by and conducted according to the regulations of the Institutional Animal Care and Use Committee (IACUC) of Drexel University College of Medicine.

Preparation of parasite antigen and reticulocyte membrane proteins. BALB/cByJ mice were infected with *P. yoelii* 17X-iRBCs. At ~15 to 20% parasitemia, blood was collected, and the iRBCs were separated by density gradient centrifugation on 70% Percoll (GE Healthcare, Piscataway, NJ). The iRBCs were washed with phosphate-buffered saline, pH 7.4 (PBS), and resuspended in 10 volumes of PBS containing 0.05% saponin (Sigma-Aldrich) for 10 min to permeabilize the erythrocyte plasma membrane. Following low-speed centrifugation at 800 × *g* for 15 min and recovery of the saponin supernatant, the pellet of intact parasites was washed with PBS-0.05% saponin and then solubilized in SDS-PAGE sample buffer. The saponin supernatant was centrifuged at 20,000 × *g* for 20 min. The resulting membrane-enriched pellet was solubilized in 20 mM Tris-HCl, pH 8.0, 50 mM NaCl, 5 mM EDTA, 1% Triton X-100, 0.5% sodium deoxycholate.

Mass spectrometry and data analysis. A 29- to 32-kDa band was purified from the *P. yoelii* 17X-infected reticulocyte membrane fraction and separated on an SDS-PAGE gel. The protein band was excised from the Coomassie blue-stained SDS-PAGE gel, destained, and digested with trypsin (Promega, Madison, WI). The recovered peptides were concentrated and desalted using ZipTip C_{18} (Millipore, Bedford, MA) and prepared for subsequent analysis using an LTQ ion trap mass spectrometer (Thermo Fisher, San Jose, CA). The mass spectrometer was interfaced with a nano-ultimate-high-performance liquid chromatography (HPLC) system (Dionex, Sunnyvale, CA). HPLC-purified peptide fractions were injected individually into the liquid chromatography-tandem mass spectrometry (LC–MS-MS) system to identify the peptides. The peptides were first concentrated using a 300-μm (inside diameter [i.d.]) by 5-mm C_{18} RP trap column (Dionex) and then separated using a 75-μm (i.d.) by 15-cm C_{18} RP analytical column (Dionex) equilibrated in 4% acetonitrile-0.1% formic acid at a 250-nl/min flow rate. Mobile phase A was 2% acetonitrile and 0.1% formic acid in water, whereas mobile phase B was 0.1% formic acid and 90% acetonitrile in water. Peptides were separated with a gradient of 4% to 50% in 60 min and 50% to 80% in 120 min and eluted directly into the mass spectrometer. The mass range in MS mode was 350 Da to 1,500 Da and in MS-MS mode was set as 100 Da to 1,500 Da. Dynamic exclusion was enabled for 180 s, and the collision energy was 30. The corresponding proteins of the tryptic peptides were identified by searching the LC–MS-MS raw data using Proteome Discoverer software (v 1.3) with the Sequest search algorithm (Thermo Electron Corporation, Waltham, MA). The Swiss-Prot database was searched within the 375-Da to 1,500-Da mass range. The search results were also verified manually to confidently identify the correct peptide sequence.

Recombinant *P. yoelii* exported protein 2. A 754-bp fragment encoding *P. yoelii* exported protein 2 (*Py*Exp2) (PY05892; PlasmoDB [http://www.plasmodb.org]) was PCR amplified from *P. yoelii* 17X cDNA using a forward primer (5′-CGCATATGACAAATATTGTAAAATGTGACGCATATAGTGATTTAG-3′) and a reverse primer (5′-GACTCGAGTTAAGCCCCATTAGCATCAGTTTCTTGATC-3′) containing NdeI and XhoI restriction sites (underlined). The amplified fragment was cloned into the NdeI/XhoI sites of the pET28 expression vector (EMD Biosciences, San Diego, CA), and the DNA sequence was confirmed. Recombinant *Py*Exp2 (r*Py*Exp2) with an N-terminal 6×His tag was expressed in *Escherichia coli* BL21 (RIL) Codon Plus cells (EMD Biosciences). Following induction of expression with 0.5 mM isopropyl β-D-1-thiogalactopyranoside (IPTG) (Fisher Scientific, Pittsburg, PA) for 4 h, bacteria were harvested and lysed in BugBuster HT protein extraction reagent (5 ml/g) containing Benzonase Nuclease (25 U/ml) and recombinant lysozyme (1 kU/ml) (EMD Biosciences) for 30 min at room temperature. The lysate was clarified by centrifugation at 20,000 × *g* for 20 min. The resulting pellet was resuspended in binding buffer (20 mM Tris-HCl, pH 7.9, 5 mM imidazole, 0.5 M NaCl) containing 6 M guanidine hydrochloride (Sigma-Aldrich, St. Louis, MO) and mixed overnight at 4°C. The material was centrifuged at 20,000 × *g* for 20 min, and the resultant soluble supernatant was used for purification of r*Py*Exp2 by nickel chelate affinity chromatography under denaturing conditions using Ni-nitrilotriacetic acid (NTA) agarose (Qiagen, Valencia, CA). The eluted r*Py*Exp2 was refolded by gradual removal of guanidine hydrochloride by dialysis in renaturing buffer (50 mM Tris-HCl, pH 8.3, 100 mM NaCl, 3 mM reduced glutathione, 0.3 mM oxidized glutathione [Sigma-Aldrich]). The final purified protein was soluble in 50 mM Tris-HCl, pH 8.3, 100 mM NaCl. Throughout these studies, protein concentrations were determined by the bicinchoninic acid (BCA) protein assay (Thermo Scientific, Rockford, IL), and purity was evaluated on Coomassie blue-stained SDS-polyacrylamide gels.

Recombinant PY04481, encoded by a member of the *pyst-a* multigene family. A 795-bp fragment of the *pyst-a* gene encoding PY04481 (PlasmoDB [http://www.plasmodb.org]) was PCR amplified from *P. yoelii* 17X cDNA using a forward primer (5′-CACATATGGAATATGCTAC AAGCCCTAATTCTTCTTC-3′) and a reverse primer (5′-GAGCGGCC GCTTACTCCTTTTTAAAAATATCCTTTAATTTGACAACA-3′) containing NdeI and NotI restriction sites (underlined). The amplified fragment was cloned into the NdeI/NotI sites of the pET28 expression vector (EMD Biosciences), and the DNA sequence was confirmed. Recombinant PY04481 (rPY04481) with an N-terminal 6×His tag was expressed in *E. coli* BL21(DE3) pLysS cells (EMD Biosciences). Bacteria were induced, harvested, and lysed as described above. The bacterial lysate was clarified by centrifugation at 20,000 × *g* for 20 min, and rPY04481 was purified from the resulting soluble fraction. A 20 to 60% ammonium sulfate fraction of the soluble bacterial lysate was resuspended in 50 mM Tris-HCl, pH 8.3, 100 mM NaCl, 8 M urea, and 50 mM dithiothreitol (DTT) (Sigma-Aldrich). The DTT was removed by dialysis into 50 mM Tris-HCl, pH 8.3, 100 mM NaCl, and 6 M urea, and rPY04481 was purified by nickel chelate affinity chromatography. The eluted rPY04481 was folded as described above by gradual removal of urea by dialysis in renaturing buffer. The final purified protein was dialyzed into 25 mM Tris-HCl, 100 mM NaCl, pH 8.0.

Antibodies. Polyclonal rabbit anti-r*Py*Exp2 and anti-rPY04481 sera were generated by Lampire Biological Laboratories (Pipersville, PA) according to their "classic-line basic" protocol. Adult New Zealand White rabbits were immunized with 200 μg of recombinant protein formulated with complete Freund's adjuvant, followed by 4 booster immunizations (200 μg each) with recombinant protein in incomplete Freund's adjuvant. Two weeks following the final immunization, the rabbits were exsanguinated and antisera were prepared. A preimmune serum sample was used as a negative control in all experiments. Mouse anti-r*Py*Exp2 sera were generated in BALB/cByJ mice. The mice were immunized three times at 3-week intervals with 10 μg of r*Py*Exp2 and 25 μg of Quil A (Accurate Chemical and Scientific Corporation, Westbury, NY) as an adjuvant. Sera from 5 mice were collected 2 weeks following the last immunization and pooled. NYLS3, an IgG1 monoclonal antibody (MAb) that recognizes *Py*Exp1 (*Py*Hep17) was a kind gift from Stefan Kappe (Seattle Biomedical Research Institute, Seattle, WA) (34). Rat anti-mouse CD71 (BD Biosciences, San Jose, CA) and mouse anti-human CD71 (eBiosciences, San Diego, CA) were used to stain mouse and human reticulocytes, respectively (35, 36). Preparations of host cell cytoplasmic and parasite-associated proteins were evaluated by immunoblotting using polyclonal rabbit anti-*P. falciparum* aldolase (Abcam, Cambridge, MA) and rabbit anti-*Py*MSP8 (37). Mouse anti-clathrin heavy chain monoclonal antibody (BF-06) (Thermo Scientific) cross-reactive to human, rabbit, mouse, bovine, and porcine clathrin heavy chain was used as a marker for host cell endocytic vesicles.

Indirect immunofluorescence assays. Indirect immunofluorescence assays (IFAs) were performed as previously described (38) with minor modifications. Blood was collected from *P. yoelii* 17X- or *P. yoelii* 17XL-infected mice and washed three times with PBS. Infected RBCs were fixed with 4% paraformaldehyde-0.0075% glutaraldehyde in PBS overnight at 4°C. The cells were then washed and permeabilized with 0.1% Triton X-100 for 10 min at room temperature, followed by treatment with 0.1 mg/ml sodium borohydride ($NaBH_4$) for 10 min. Nonspecific binding was blocked with PBS containing 5% nonfat dry milk for 1 h, followed by incubation with mouse anti-r*Py*Exp2 sera (1:400) or normal mouse sera (1:400) overnight at 4°C. The primary antibody was detected by using fluorescein-conjugated goat anti-mouse IgG(H+L) (1:400; Life Technologies, Grand Island, NY). Parasite nuclei were stained using SlowFade Gold containing 4,6-diamidino-2-phenylindole (DAPI) (Invitrogen).

For quantitation of cytoplasmic Exp2 vesicle-positive RBCs, *P. yoelii* 17X-infected reticulocytes were fixed as described above and costained with mouse anti-r*Py*Exp2 (1:400) and rat anti-mouse CD71 (1:200) sera. Fluorescein-conjugated goat anti-mouse IgG(H+L) (Life Technologies) and rhodamine-conjugated goat anti-rat IgG (eBiosciences) were used as secondary antibodies. The number of Exp2 vesicle-positive cells per 500 *P. yoelii*-infected cells containing rings, trophozoites, or schizonts was determined for each mouse ($n = 5$) and expressed as percent positive. The data are presented as the mean and standard deviation (SD) for each group.

For comparative studies, *P. yoelii* 17X-infected reticulocytes were isolated from mice on day 9 postinfection (parasitemia, 9.2% ± 4.3%), while *P. yoelii* 17XL-infected mature RBCs were isolated on day 4 postinfection (parasitemia, 11.2% ± 3.0%). To isolate *P. yoelii* 17XL-infected reticulocytes, mice were treated by intraperitoneal (i.p.) injection with phenylhydrazine (Sigma; 0.55 mg/mouse/day) on days −5, −3, −2, and −1 prior to infection. The resulting mild anemia and compensatory increase in reticulocytes (39) were monitored by counting the polychromatophilic RBCs on thin blood smears stained by Giemsa. *P. yoelii* 17XL-infected reticulocytes were isolated from the phenylhydrazine-treated mice on day 4 postinfection (parasitemia, 7.2% ± 5.3%). Cytoplasmic Exp2-positive vesicles were identified by immunofluorescence staining using mouse anti-r*Py*Exp2 and rat anti-mouse CD71 sera as described above. The number of Exp2 vesicle-positive cells (mature RBCs or reticulocytes) per 500 *P. yoelii*-infected cells per mouse (5 mice/group) was determined and expressed as percent positive. The data are presented as the mean and SD for each group. The statistical significance of differences was determined by two-tailed, unpaired Student's *t* test. Probability (*P*) values of <0.05 were considered significant.

Wide-field fluorescence microscopy. Two-dimensional immunofluorescence images (×1,000 magnification) were obtained by using an Olympus BX60 fluorescence microscope (Olympus America, Inc., Melville, NY) and a Sensicam QE high-performance camera system (Cooke Corporation, Romulus, MI). Images were captured and processed using Slidebook 5.0 software (Intelligent Imaging Innovations Inc., Denver, CO). For three-dimensional (3D) volume rendering, z-stacks were taken using a 200-nm step size, and deconvolution was performed using the "no neighbor" setting.

Structured-illumination superresolution microscopy. Three-dimensional structured-illumination microscopy (3D-SIM) was performed in the Cell Imaging Center of Drexel University, Philadelphia, PA. 3D-SIM utilized the DeltaVision OMX V4 (Applied Precision-GE Healthcare, Issaquah, WA) imaging platform, which enables the imaging of cells and tissue sections at a resolution better than the theoretical resolution limit (~200 nm) of light microscopy. The DeltaVision OMX is equipped with the Blaze SIM module, which enables 3D superresolution imaging at ~120-nm lateral and ~300-nm axial resolution using standard dyes and fluorescent tags. The 3D-SIM instrument is equipped with an Olympus Plan Apo N 60×/1.42-numerical-aperture (NA) objective; three liquid-cooled scientific complementary metal oxide semiconductor (sCMOS) cameras; and 405-, 445-, 488-, 568-, and 642-nm diode lasers. Multichannel images were captured simultaneously using sCMOS cameras, and 3D-SIM images were sectioned using a 125-nm z-step. Raw images were acquired and 3D projections were reconstructed using SoftWorx 5.0 software (Applied Precision-GE Healthcare).

Bodipy TR ceramide staining. Bodipy TR ceramide (Life Technologies) was used to stain membranes in *P. yoelii* 17X-infected cells as described previously (40) with some modifications. Briefly, 1×10^8 cells were washed three times with RPMI 1640 and labeled with 20 μM Bodipy TR Ceramide for 30 min at 37°C. The labeled cells were washed and used to prepare thin blood smears. The labeled iRBCs were then fixed in 1% paraformaldehyde in PBS for 20 min, followed by permeabilization with PBS-0.1% saponin for 10 min. Nonspecific binding was blocked by incubation for 30 min with PBS containing 0.1% bovine serum albumin (BSA) and 0.05% saponin. Mouse anti-r*Py*Exp2 serum (1:200) was diluted in PBS-0.01% saponin and incubated at 37°C for 1 h. Subsequent staining with secondary antibodies and fluorescence microscopy were performed as described above.

Quantitative analysis of Exp2 expression in *P. yoelii* 17X- versus *P. yoelii* 17XL-infected RBCs. BALB/cByJ mice were infected with either *P. yoelii* 17X or *P. yoelii* 17XL, and iRBCs were isolated as described above

and resuspended in 10 volumes of PBS-0.05% saponin. Intact parasites were separated from the host cell cytoplasmic fraction by low-speed centrifugation at 800 × *g* for 15 min and resuspended in 10 volumes of SDS-PAGE sample buffer. For the initial immunoblot analysis, equal volumes of the parasite-associated fractions from *P. yoelii* 17X- and *P. yoelii* 17XL-iRBCs were analyzed. In the same assay, a 5-fold-larger volume of the host cell cytoplasmic fraction was analyzed to compensate for the lower concentrations of *Py*Exp2 expected. The saponin-released host cell cytoplasmic fractions obtained from *P. yoelii* 17X- and *P. yoelii* 17XL-infected RBCs were further separated into soluble and particulate fractions by centrifugation at 20,000 × *g* for 45 min. To compare the concentrations of Exp2 in each fraction, the particulate material was resuspended in SDS-PAGE sample buffer in a volume equal to that of the starting material. For the immunoblot analysis, equal volumes of each fraction were analyzed.

Transgenic parasites. (i) *Py*Exp2 knockout construct. A double-crossover homologous-recombination strategy was used in an effort to knock out the *pyexp2* gene. The pB3D-3M plasmid (obtained from Lawrence Bergman, Drexel University College of Medicine, Philadelphia, PA) containing the *Toxoplasma gondii dhfr-ts* (*Tg-dhfr-ts*) pyrimethamine resistance cassette as a selectable marker was used to generate the targeting construct. Two fragments, 292 bp and 331 bp, flanking the 5′ end and 3′ end of the *pyexp2* gene, respectively, were PCR amplified from *P. yoelii* 17X genomic DNA. The 5′ fragment was cloned into KpnI and HindIII sites, while the 3′ fragment was cloned into BamHI and NotI sites to generate the plasmid pB3D-3M-ΔExp2. The plasmid DNA was isolated using the Qiagen Plasmid Mega kit (Qiagen) and digested with KpnI and NotI to release the fragment containing the drug resistance cassette flanked by 5′-end and 3′-end sequences. Ten micrograms of the linear DNA fragment was used for transfection of *P. yoelii* parasites.

(ii) *Py*Exp2-3HA construct. To tag the *pyexp2* gene, a single-crossover recombination strategy was used. The pSE02-3HA plasmid (Lawrence Bergman, Drexel University College of Medicine) containing the *Tg-dhfr-ts* pyrimethamine resistance cassette as a selectable marker was used to generate the tagging construct. A 495-bp fragment from the 3′ end of the *pyexp2* gene was amplified from *P. yoelii* 17X genomic DNA and cloned into pSE02-3HA preceding the triple-hemagglutinin (HA) sequence, resulting in the construct pSE02-3′Exp2-3HA. Plasmid DNA was isolated as described above and linearized by digestion with EcoRI prior to transfection.

(iii) Transfection and selection of transgenic parasites. Blood was collected from *P. yoelii* 17X-infected mice at a parasitemia of ~10%, washed, and incubated at 37°C for 4 h in RPMI 1640, 20% fetal bovine serum, 25 mM HEPES, pH 7.0, 7.5% $NaHCO_3$, and penicillin-streptomycin (100 U/ml). The resulting schizont-enriched parasites were isolated by density gradient centrifugation on 70% Percoll. Transfection was performed using the Amaxa (Lonza, Basel, Switzerland) Basic Parasite Nucleofector kit 2 as described previously (41). Briefly, 10 μg of linearized plasmid was added to 100 μl of Nucleofector solution and transferred to a cuvette, pulsed (U33 program; Amaxa [Lonza, Basel, Switzerland] Nucleofector), and injected intravenously into a recipient mouse. At least two independent transfections were performed for each construct each time. Starting at 24 h postinfection, the mice were treated i.p. with 0.8 mg kg of body weight^{-1} pyrimethamine (Sigma-Aldrich) daily until parasites were no longer detectable (42). Once drug-resistant parasites appeared, the parasites were passaged into a new mouse by intravenous (i.v.) injection to increase parasite numbers sufficiently for DNA isolation and antigen preparation.

***P. falciparum* culture and reticulocyte invasion assay.** *P. falciparum* FVO (ATCC, Manassas, VA) parasites were grown in complete medium containing RPMI 1640 (Sigma-Aldrich) supplemented with 2 mM L-glutamine, 10 μg/ml hypoxanthine, 20 mM HEPES, pH 7.4, 25 mM sodium bicarbonate, 20 mM glucose, 100 U/ml penicillin-streptomycin, and 0.25% Albumax II (Life Technologies) at 2% hematocrit of O^+ human RBCs (Interstate Blood Bank, Inc., Memphis, TN) in a mixture of 90% N_2, 5% CO_2, and 5% O_2. Parasite growth was synchronized by two successive treatments 12 h apart with an equal volume of 0.5 M L-alanine in 10 mM HEPES, pH 7.5, for 10 min at 37°C. Mature-stage parasites were enriched by density gradient centrifugation on 70% Percoll and used for reticulocyte invasion assays. Human cord blood (Zen-Bio, Research Triangle Park, NC) was used as a source of reticulocytes. The cord blood was washed three times in complete medium, and reticulocytes were enriched by density gradient centrifugation on 70% Percoll at 2,000 × *g* for 20 min. The reticulocyte layer was removed, and the cells were washed with complete medium. The enriched *P. falciparum* FVO schizonts were mixed with reticulocyte-enriched cord blood at a 1:1 ratio and cultured for 48 h. Cells were harvested at 16-, 24-, and 36-hour time points and fixed with 4% formaldehyde-0.0075% glutaraldehyde in PBS for immunofluorescence assays. Parasite invasion of reticulocytes and normocytes was evaluated by Giemsa-stained thin smears.

RESULTS

Expression, purification, and analysis of recombinant *P. yoelii* Exp2. As part of ongoing studies of parasite proteins exported across the PVMs of reticulocyte-restricted malaria parasites, a proteomic analysis of *P. yoelii* 17X proteins associated with a fraction enriched in host reticulocyte plasma and cytoplasmic membranes was performed. Coomassie blue-stained SDS-PAGE analysis of the host reticulocyte membrane fractions from uninfected and *P. yoelii* 17X-infected RBCs showed a significant enrichment of host RBC plasma membrane proteins, as seen by the presence of spectrin dimers and band 3 (see Fig. S1A, lanes 1 and 2, in the supplemental material). In addition, several unique protein bands were present in the *P. yoelii* 17X-infected reticulocyte membrane fraction compared to that from uninfected cells, and they were presumably of parasite origin (see Fig. S1A, lane 2, in the supplemental material). Using antibodies against *P. yoelii* merozoite surface protein 8 (*Py*MSP8), an abundant glycosylphosphatidylinositol (GPI)-anchored membrane protein of *P. yoelii* trophozoites and schizonts (37), the absence of parasite plasma membrane proteins in the reticulocyte membrane fraction was confirmed (see Fig. S1B in the supplemental material).

*Py*Exp2 (PY05892) was identified as 1 of 9 *P. yoelii* proteins migrating on SDS-polyacrylamide gels at ~29 to 32 kDa (see Fig. S1C in the supplemental material). The protein sequence of *Py*Exp2 is characterized by an N-terminal signal sequence and an abundance of charged residues near the C terminus that include several aspartate residues (Fig. 1A). *Py*Exp2 does not possess a PEXEL motif or a predicted transmembrane domain. It is well conserved among *Plasmodium* spp., showing some variability in the C-terminal acidic region (Fig. 1B). To characterize Exp2 in *P. yoelii*, r*Py*Exp2 was produced in *E. coli* using a T7 RNA polymerase expression system. The recombinant protein was purified from an insoluble fraction of the bacterial lysate by nickel chelate affinity chromatography and refolded. Analysis by SDS-PAGE showed that purified r*Py*Exp2 migrated as a prominent band of 30 to 31 kDa (Fig. 1C). Polyclonal antisera generated against purified r*Py*Exp2 were tested for specificity by immunoblotting. Both rabbit and mouse anti-r*Py*Exp2 antibodies detected the native protein of ~28 to 29 kDa in a *P. yoelii* 17X blood-stage lysate (Fig. 1D and E), consistent with the predicted molecular mass of mature *Py*Exp2.

***Py*Exp2 is localized to the PVM and membrane-bound vesicles in the host reticulocyte cytoplasm.** To determine the localization of *Py*Exp2, blood was collected from *P. yoelii* 17X-infected mice at day 9 postinfection, when the parasitemia was ~10%. Indirect immunofluorescence assays using mouse anti-r*Py*Exp2

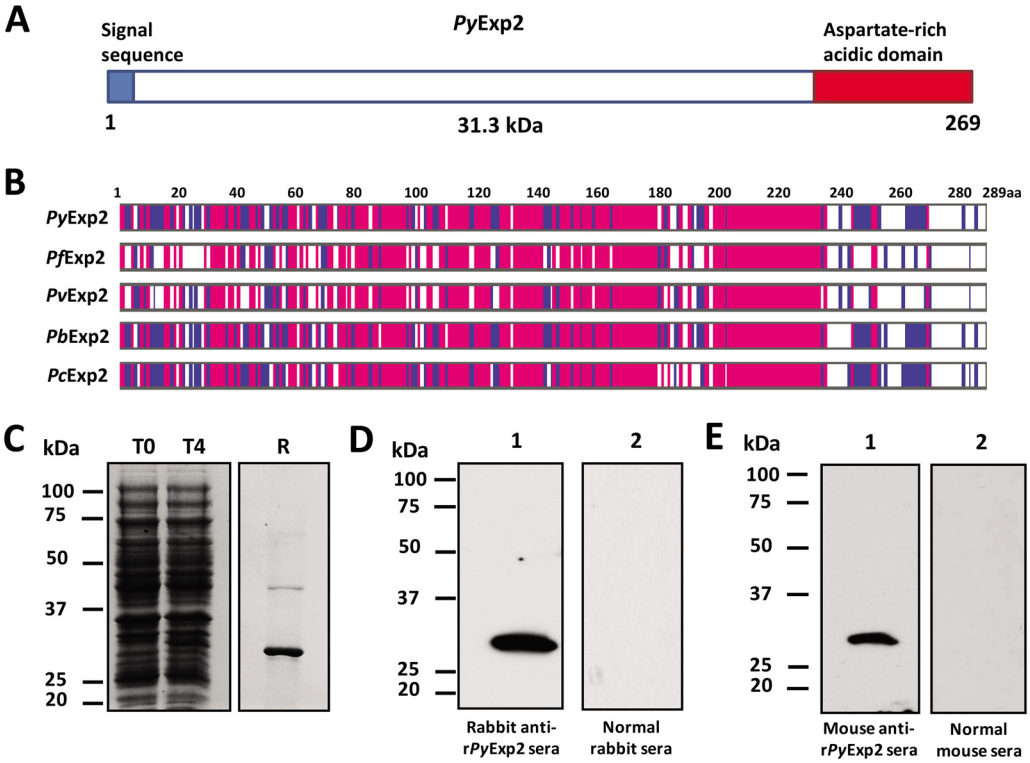

FIG 1 Expression and purification of r*Py*Exp2. (A) Schematic structure of *Py*Exp2 indicating the N-terminal signal sequence (blue) and the location of the C-terminal charged domain (red). (B) Alignment of the deduced amino acid (aa) sequence of *Py*Exp2 with those of Exp2 proteins in other *Plasmodium* spp. Blue, identical residues in at least two sequences; pink, identical residues in all five sequences. (C) Coomassie blue-stained SDS-PAGE gel showing *E. coli* lysate at the time of IPTG induction (T0) and 4 h postinduction (T4) and recombinant protein (R) (3 μg) purified by nickel chelate affinity chromatography. (D) Immunoblot analysis of *P. yoelii* 17X parasite antigen lysate (5 μg) probed with rabbit anti-r*Py*Exp2 sera (lane 1) or normal rabbit sera (lane 2). (E) Immunoblot analysis of *P. yoelii* 17X parasite antigen lysate (5 μg) probed with mouse anti-r*Py*Exp2 sera (lane 1) or normal mouse sera (lane 2). Molecular mass markers are indicated.

antibodies showed that *Py*Exp2 was expressed in all blood stages and localized to the PVM, but also to vesicles in the reticulocyte cytoplasm that appeared to be distinct from the PVM (Fig. 2A). These *Py*Exp2-positive vesicles were clearly detected in the cytoplasm of RBCs containing early ring-stage parasites and in RBCs harboring the later trophozoite and schizont stages. Notably, *Py*Exp2-positive vesicles were also seen at some distance from the PVM, sometimes in close association with the host reticulocyte plasma membrane (Fig. 2A). High-resolution images of these *Py*Exp2-positive vesicles were obtained by 3D-SIM (43). As shown by 3D-SIM (Fig. 2B), *Py*Exp2-positive vesicles appear as discrete spherical structures in the reticulocyte cytoplasm. Importantly, rotation of the 3D-SIM projection (see Movie S1 in the supplemental material) clearly shows that the cytoplasmic *Py*Exp2-positive vesicles are independent of both the PVM surrounding the intracellular parasite and any TVN in the reticulocyte cytoplasm. To determine the stage-specific distribution of *Py*Exp2-positive vesicles, the number of Exp2 vesicle-positive cell per 500 *P. yoelii*-infected cells from each of five mice was determined. Stage-specific analysis showed that 32.5% of iRBCs at the trophozoite stage contained *Py*Exp2-positive vesicles, whereas 12.8% and 2.7% of iRBCs at the ring and schizont stages, respectively, were positive for *Py*Exp2 vesicles (Fig. 2C).

*Py*Exp2-positive vesicular structures were examined by labeling with Bodipy TR ceramide, a lipid analogue used to stain cellular membranous components (44). As expected, Bodipy labeled various membranes within the parasite, the PVM, and both punctate and tubular structures in the infected reticulocyte cytoplasm. Colabeling of a subset of Bodipy-stained structures with anti-r*Py*Exp2 antibodies showed *Py*Exp2 associated with membrane-bound vesicles (Fig. 2D, i; see Movie S2 in the supplemental material). Colocalization using 3D-SIM shows that an isolated, spherical *Py*Exp2-positive vesicle in the reticulocyte cytoplasm is also labeled with Bodipy TR ceramide (Fig. 2D, ii, arrow; see Movie S3 in the supplemental material). There are numerous Bodipy-positive but *Py*Exp2-negative tubular/vesicular structures in the reticulocyte cytoplasm that are reminiscent of Maurer's clefts in *P. falciparum* (12) and caveola-like structures in *P. vivax*-infected reticulocytes (30). They may also include host cell-derived components and endocytic vesicles that remain from an earlier stage of erythroid development.

The localization of *Py*Exp2 was independently verified by adding a triple-HA tag at the 3′ end of the endogenous *pyexp2* using a single-recombination strategy (see Fig. S2 in the supplemental material). Expression of a *Py*Exp2-3HA fusion protein of the predicted size (37 kDa) in the transgenic parasite line was confirmed by immunoblot analysis using anti-r*Py*Exp2 antibodies and an anti-HA monoclonal antibody (Fig. 3A). Importantly, immunofluorescence staining showed that the C-terminal HA tag did not alter the localization of *Py*Exp2 to the PVM or to the vesicular structures in the infected reticulocyte cytoplasm (Fig. 3B). These data provide further support for the presence of distinct spherical

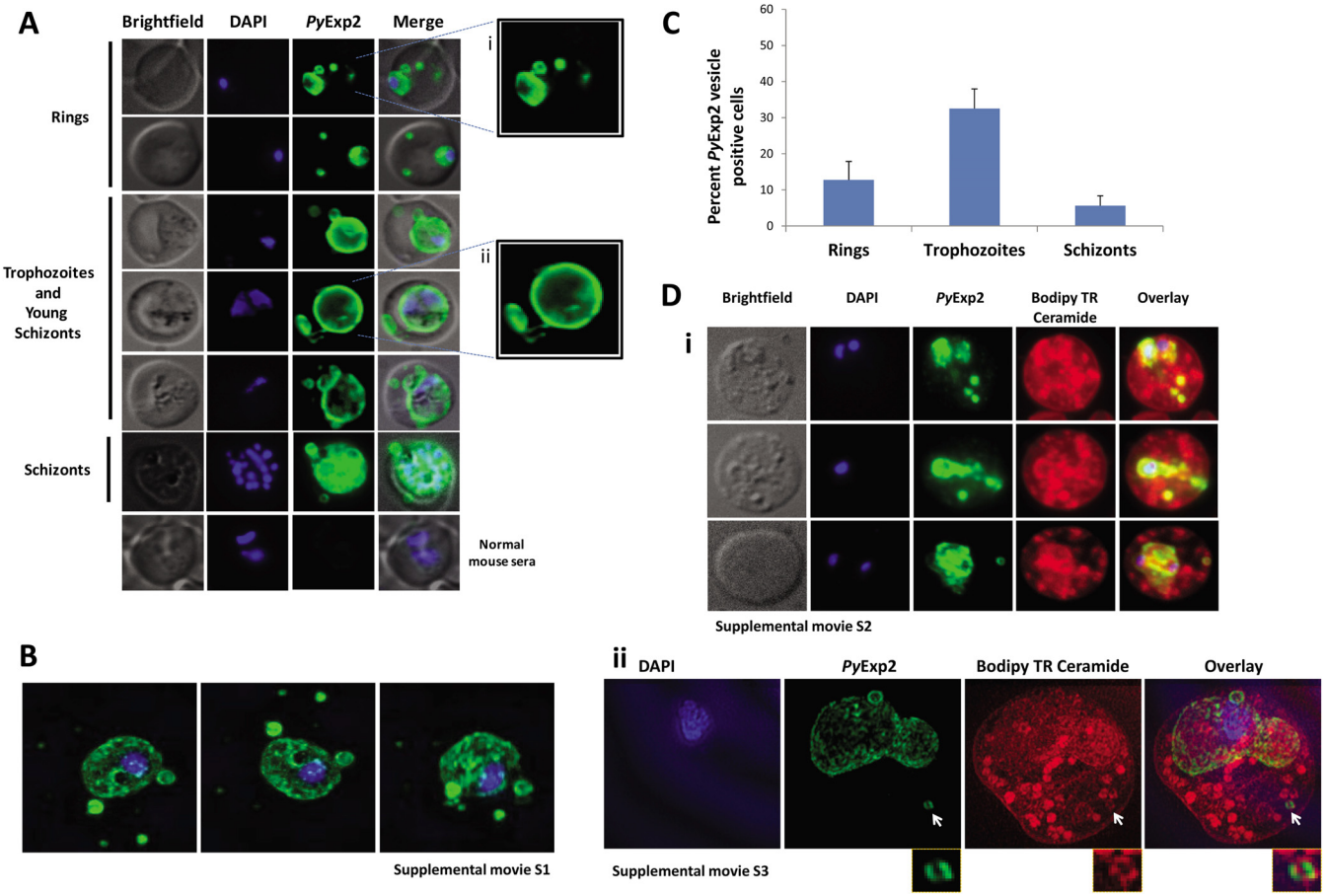

FIG 2 *Py*Exp2 is localized to the PVM and membranous vesicles in the cytoplasm of *P. yoelii* 17X-infected RBCs. (A) Localization of *Py*Exp2 (green) in *P. yoelii* 17X-infected reticulocytes was evaluated by immunofluorescence assay using mouse anti-r*Py*Exp2 sera. The enlarged images on the right show distinct *Py*Exp2-positive vesicles in a ring-stage parasite (i) and trophozoite/young-schizont stage parasites (ii). (B) Representative 3D-SIM sections showing the organization of *Py*Exp2-positive vesicles. A 3D rotational view is shown in Movie S1 in the supplemental material. (C) Percentages of ring, trophozoite, and schizont stages containing *Py*Exp2-positive vesicles in *P. yoelii* 17X-infected reticulocytes. The percentages are expressed as means and SD. (D) (i) Immunofluorescence images showing dual labeling with Bodipy TR ceramide (red) and *Py*Exp2 (green) in *P. yoelii* 17X-infected RBCs. A rotational 3D volume view of z-stacks corresponding to the images in the bottom row is shown in Movie S2 in the supplemental material. (ii) 3D-SIM sections showing individual channels and overlay of DAPI (blue), *Py*Exp2 (green), and Bodipy TR ceramide (red). The arrows identify a *Py*Exp2-positive vesicle in the reticulocyte cytoplasm costained with Bodipy TR ceramide. A 3D rotational view is shown in Movie S3 in the supplemental material. The cells were stained in suspension with Bodipy TR ceramide, followed by fixation on glass slides, and probed with mouse anti-r*Py*Exp2 sera as described in Materials and Methods. DAPI was used to stain parasite nuclei (blue).

*Py*Exp2-positive vesicles in the cytoplasm of *P. yoelii* 17X-infected reticulocytes.

***Py*Exp1, *Py*pAg-1 (PY06203), and PY04481 are associated with *Py*Exp2-positive vesicles.** To determine if other PVM proteins were also associated with *Py*Exp2-positive vesicles, the localization of *Py*Exp2 and *Py*Exp1/Hep17 was evaluated by immunofluorescence assay. As expected, *Py*Exp1 was found primarily associated with the PVM, colocalizing with *Py*Exp2 (Fig. 4). In addition, *Py*Exp2-positive vesicles also costained with the anti-*Py*Exp1 MAb, suggesting that these cytoplasmic vesicles were derived from the PVM. To determine if *Py*Exp2-positive vesicles can carry protein cargo, colocalization assays were performed using antibodies for two exported *P. yoelii* proteins. *Py*pAg-1 (PY06203) is a tryptophan-rich protein exported into the host cytoplasm and associated with the membranes of *P. yoelii*-iRBCs (45). Proteins encoded by members of the *pyst-a* gene family contain predicted signal peptides (46) and have been localized to the cytoplasmic face of the erythrocyte plasma membrane (47). A member of the *pyst-a* family, PY04481, was also identified by the proteomic analysis of *P. yoelii* 17X proteins associated with host reticulocyte plasma and cytoplasmic membranes (see Fig. S1 in the supplemental material). Polyclonal rabbit antibodies were generated against purified rPY04481 (see Fig. S3 in the supplemental material). Colocalization of *Py*Exp2 with the exported proteins *Py*pAg-1 and PY04481 was assessed by immunofluorescence assay. As shown in Fig. 5, both *Py*pAg-1 and PY04481 localized with *Py*Exp2-positive vesicles in the reticulocyte cytoplasm, although not exclusively. These data suggest that *Py*Exp2-positive vesicles have the capacity to transport *P. yoelii* proteins through the host RBC cytoplasm.

***Py*Exp2-positive vesicles form predominantly in reticulocytes infected with lethal or nonlethal *P. yoelii*.** Initial results demonstrated *Py*Exp2-positive vesicles in the cytoplasm of RBCs infected with reticulocyte-prone, nonlethal *P. yoelii* 17X parasites. To determine if such vesicles are also induced upon infection of mature erythrocytes, the localization of *Py*Exp2 was evaluated in

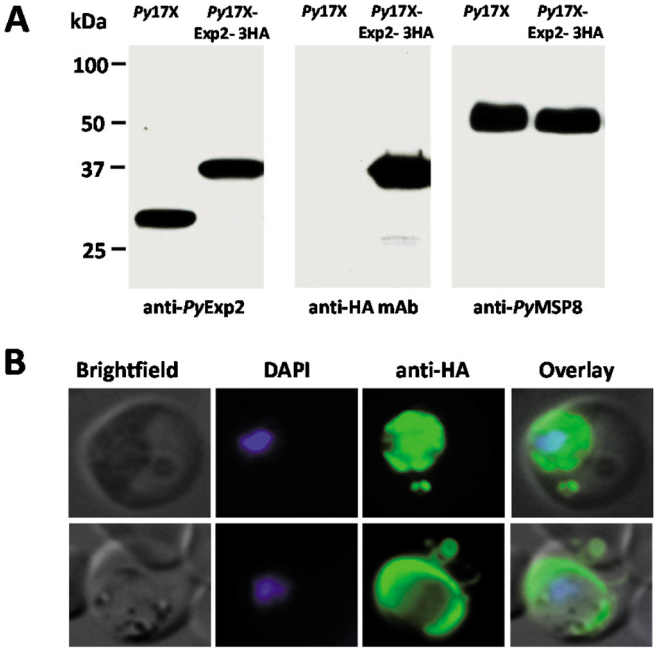

FIG 3 Localization of *Py*Exp2 containing a C-terminal HA tag is unaltered in *P. yoelii* 17X-infected RBCs. (A) Immunoblot analysis of *P. yoelii* 17X parasite lysate and transgenic *P. yoelii* 17X-Exp2-3HA parasite lysate probed with rabbit anti-r*Py*Exp2 sera, mouse anti-HA monoclonal antibody, or rabbit anti-r*Py*MSP8 sera. Parasites obtained by saponin lysis of infected RBCs were solubilized in SDS-PAGE sample buffer, and equal volumes of parasite lysate were loaded on the gel. Molecular mass markers are indicated. (B) Immunofluorescence images showing localization of *Py*Exp2-3HA fusion protein (green) in RBCs infected with transgenic *P. yoelii* 17X-Exp2-3HA parasites using mouse anti-HA monoclonal antibody. DAPI was used to stain the parasite nuclei (blue).

RBCs infected with lethal *P. yoelii* 17XL parasites. Interestingly, immunofluorescence assays showed that *Py*Exp2 in *P. yoelii* 17XL-infected mature RBCs is tightly localized to the PVM with no staining of vesicles in the erythrocyte cytoplasm (see Fig. S4 in the

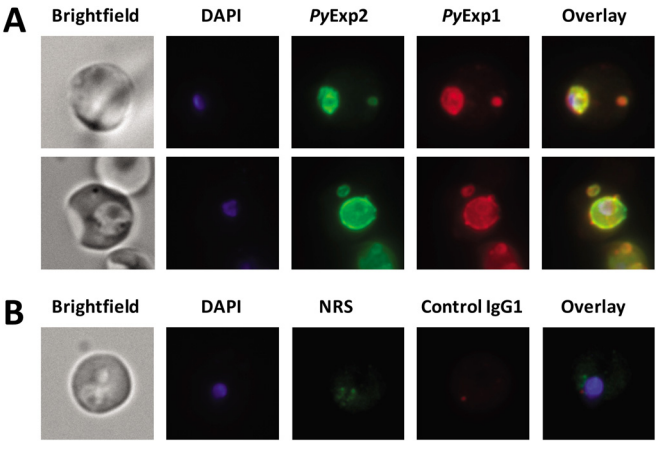

FIG 4 *Py*Exp1 colocalizes with *Py*Exp2 on the PVM and on cytoplasmic vesicles in *P. yoelii* 17X-infected RBCs. (A) Immunofluorescence images showing colocalization of *Py*Exp2 (green) and *Py*Exp1 (red) using rabbit anti-r*Py*Exp2 sera and a mouse MAb specific for *Py*Exp1, respectively. (B) Normal rabbit sera (NRS) and a mouse IgG1 myeloma protein were used as controls. DAPI was used to stain the parasite nuclei (blue).

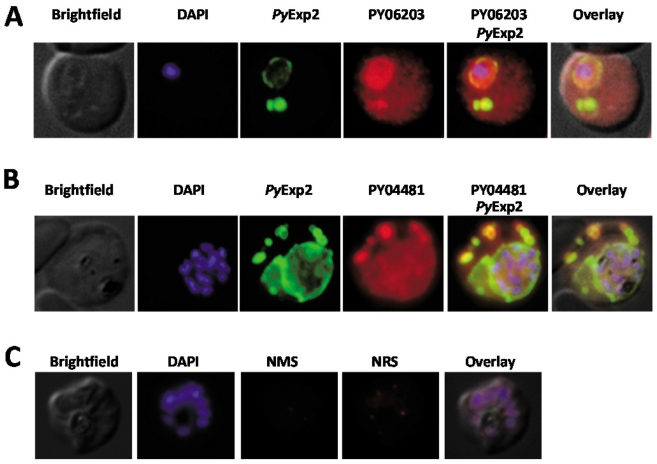

FIG 5 *Pyp*Ag-1 (PY06203) and PY04481 localize within *Py*Exp2-positive vesicles in *P. yoelii* 17X-infected RBCs. (A) Immunofluorescence images showing colocalization of *Py*Exp2 (green) and *Pyp*Ag-1 (PY06203) (red) using mouse anti-r*Py*Exp2 sera and rabbit anti-*Pyp*Ag-1 sera, respectively. (B) Immunofluorescence images showing colocalization of *Py*Exp2 (green) and PY04481 (red) using mouse anti-r*Py*Exp2 sera and rabbit anti-rPY04481 sera, respectively. (C) Normal mouse sera (NMS) and normal rabbit sera (NRS) were used as controls. DAPI was used to stain the parasite nuclei (blue).

supplemental material). While lethal *P. yoelii* 17XL predominantly infects mature RBCs in circulation, this strain readily invades reticulocytes when available (39). To determine if the host cell environment influences vesicle formation, the localization of *Py*Exp2 was evaluated in mature RBCs and reticulocytes infected with the lethal *P. yoelii* 17XL in comparison to *P. yoelii* 17X-infected reticulocytes. The reticulocyte marker CD71 (transferrin receptor) was used to differentiate mature RBCs from reticulocytes. CD71 is highly expressed on the surface of reticulocytes but is gradually lost during reticulocyte maturation and is absent in mature RBCs (48) (Fig. 6A; see Fig. S5 in the supplemental material).

As shown in Fig. 6A, *Py*Exp2-positive vesicles were absent in CD71-negative, mature RBCs infected with *P. yoelii* 17XL. To increase the number of circulating reticulocytes early during infection, mice were pretreated with phenylhydrazine to induce a mild anemia and erythropoiesis (39). In *P. yoelii* 17XL-infected, CD71-positive reticulocytes, *Py*Exp2-positive vesicles were readily observed in the host cytoplasm, similar to nonlethal *P. yoelii* 17X-infected reticulocytes (Fig. 6A). Visualization by 3D-SIM confirmed the presence of *Py*Exp2-positive vesicles in *P. yoelii* 17XL-infected reticulocytes (CD71 positive) but not mature RBCs (CD71 negative) (Fig. 6A; see Movies S4 and S5 in the supplemental material). Again, 3D-SIM demonstrated that these *Py*Exp2-positive vesicles were not contiguous with the PVM. While 41.1% of *P. yoelii* 17X-infected reticulocytes contained *Py*Exp2-positive vesicles, only 1.8% of *P. yoelii* 17XL-infected mature RBCs stained positively for *Py*Exp2 vesicles. However, when *P. yoelii* 17XL shifted to infection of reticulocytes, vesicle formation markedly increased, with 21.3% of *P. yoelii* 17XL-infected reticulocytes now containing *Py*Exp2-positive vesicles (Fig. 6B). These data suggest that the formation of Exp2-positive vesicles is not parasite strain specific but depends on host cell factors uniquely associated with reticulocytes. To rule out the possibility that these vesicles were formed by endocytosis of the reticulocyte plasma membrane (49), colocalization of *Py*Exp2 with host clathrin was evaluated.

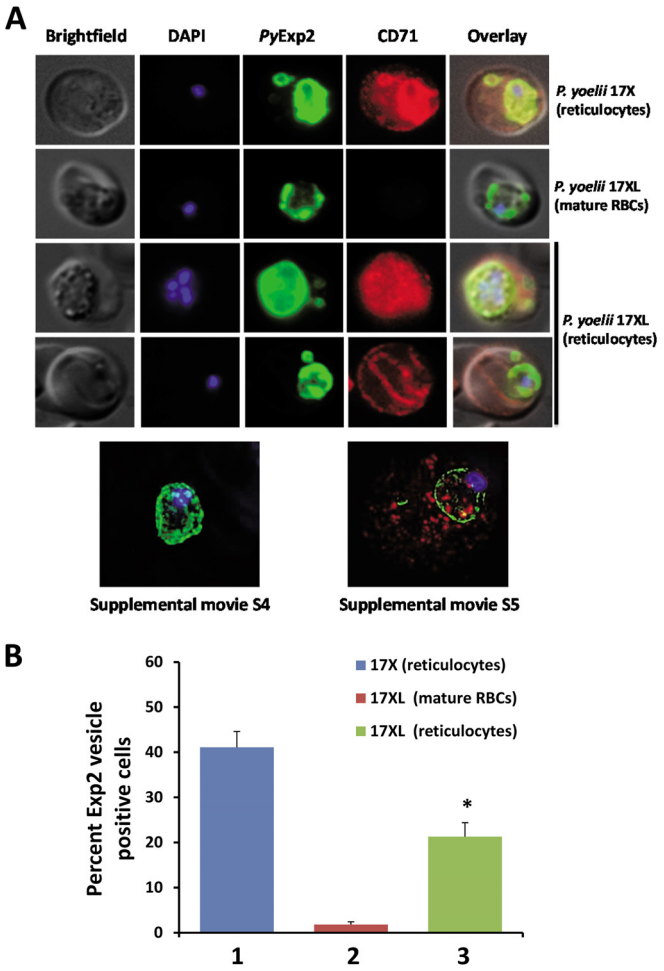

FIG 6 *Py*Exp2-positive vesicles are predominantly associated with reticulocytes infected with *P. yoelii*. (A) Immunofluorescence images showing costaining of *Py*Exp2 (green) and CD71 (red) in RBCs infected with the *P. yoelii* 17X or *P. yoelii* 17XL strain. Shown at the bottom are representative sections of a 3D-SIM image of a *P. yoelii* 17XL-infected mature RBC (CD71 negative) and a *P. yoelii* 17XL-infected reticulocyte (CD71 positive); rotational 3D renderings are shown in Movies S4 and S5 in the supplemental material. (B) Percentages of infected cells containing *Py*Exp2-positive vesicles in *P. yoelii* 17X-infected reticulocytes (1), *P. yoelii* 17XL-infected mature RBCs (2), or *P. yoelii* 17XL-infected reticulocytes (3). The percentages are expressed as means and SD. *, statistically significant difference ($P < 0.05$) between groups 2 and 3.

*Py*Exp2-positive vesicles did not colocalize with mouse clathrin in the *P. yoelii* 17X-infected reticulocytes. *Py*Exp2-positive vesicles do not represent endocytic clathrin-coated vesicles (see Fig. S6 in the supplemental material).

Quantitative and qualitative differences in host cell-dependent expression of *Py*Exp2 were further evaluated. *P. yoelii* 17X-infected reticulocytes and *P. yoelii* 17XL-infected mature RBCs were treated with 0.05% saponin, and released intact parasites were separated from the host cell cytoplasmic fraction by low-speed centrifugation. Immunoblot assays with antibodies against *Py*MSP8, a GPI-anchored parasite plasma membrane (PPM) protein (37), or the glycolytic enzyme aldolase, a cytosolic protein in *Plasmodium* (50), were used to evaluate the integrity of the PPM. *Py*MSP8 and *P. yoelii* aldolase were predominantly associated with the intracellular parasite, with only a low level of *P. yoelii* aldolase present in the host cell cytoplasmic fraction (Fig. 7A and B). As such, the PPM remained largely intact during saponin treatment.

As shown by immunoblot analysis (Fig. 7C), no significant differences in *Py*Exp2 protein levels were seen in the parasite-associated fraction or initial host cell cytoplasmic fraction from *P. yoelii* 17X- and 17XL-iRBCs. Comparable amounts of lysate from *P. yoelii* 17X- and *P. yoelii* 17XL-infected RBCs were loaded, as evident from immunoblot analysis to detect *Py*MSP8 and *P. yoelii* aldolase (Fig. 7A and B). However, when the host cell cytoplasmic fraction was further subjected to high-speed centrifugation (20,000 × *g*), *Py*Exp2 from the cytoplasm of *P. yoelii* 17XL-iRBCs was found primarily in the pelleted particulate material (Fig. 7D). In marked contrast, *Py*Exp2 from the cytoplasm of *P. yoelii* 17X-infected reticulocytes was proportionally distributed between the soluble supernatant and pelleted particulate material. Exp2 in *P. falciparum* has been shown to be strongly associated with the PVM, with a predicted model of an ~600- to 700-kDa homo-oligomeric Exp2 pore anchored to the PTEX macromolecular complex (23). The presence of *Py*Exp2 in an insoluble fraction of the host cytoplasm released by saponin treatment is consistent with formation of a similar PVM-associated *Py*Exp2-PTEX complex. However, the remaining soluble fraction of the cytoplasm from infected reticulocytes, but not mature RBCs, also contains a second, distinct form of *Py*Exp2.

***Py*Exp2 is essential in lethal and nonlethal *P. yoelii* blood-stage parasites.** To assess the importance of *Py*Exp2 for the growth of *P. yoelii* blood-stage parasites *in vivo*, a targeted disruption of the *pyexp2* gene was attempted. The targeting construct was designed to recombine by double crossover at the 5′ and 3′ ends of the gene and to replace the endogenous *pyexp2* gene with the *Tg-dhfr-ts* selectable marker (see Fig. S7 in the supplemental material). Following transfection and positive selection, drug-resistant parasites were never obtained in five independent attempts with *P. yoelii* 17X and two independent attempts with *P. yoelii* 17XL. In two additional transfections of *P. yoelii* 17X, drug-resistant parasites were obtained, but the endogenous gene was intact, as revealed by diagnostic PCR with the resistance marker integrated elsewhere in the genome (data not shown). The *pyexp2* gene could not be deleted in *P. yoelii*. The *pyexp2* gene was accessible for genetic manipulation, as a triple-HA tag was successfully fused to the 3′ end of the endogenous *pyexp2* (Fig. 3; see Fig. S2A in the supplemental material). The 3′ integration in the *pyexp2* genomic locus was confirmed by diagnostic PCR (see Fig. S2B in the supplemental material). Combined, these results indicate that *Py*Exp2 is essential for *in vivo* growth of both lethal and nonlethal strains of *P. yoelii*.

Exp2-bound vesicles are formed in reticulocyte-prone *P. berghei* ANKA parasites. The rodent malaria parasite *P. berghei* ANKA has been widely used as an experimental model of cerebral malaria (51, 52). *P. berghei* ANKA has a predilection for reticulocytes when available but can also invade mature RBCs (53, 54). *P. berghei* and *P. yoelii* Exp2 share 94% identity and 98% similarity at the amino acid level. To evaluate the formation of Exp2-positive vesicles in reticulocytes infected with other species of malarial parasites, *P. berghei* Exp2 (*Pb*Exp2) expression was localized in iRBCs by immunofluorescence using anti-r*Py*Exp2 antibodies. As shown in Fig. 8, *Pb*Exp2-positive vesicles in the host cell cytoplasm were frequently associated with CD71-positive reticulocytes but were lacking in most CD71-negative mature RBCs infected with *P. ber-*

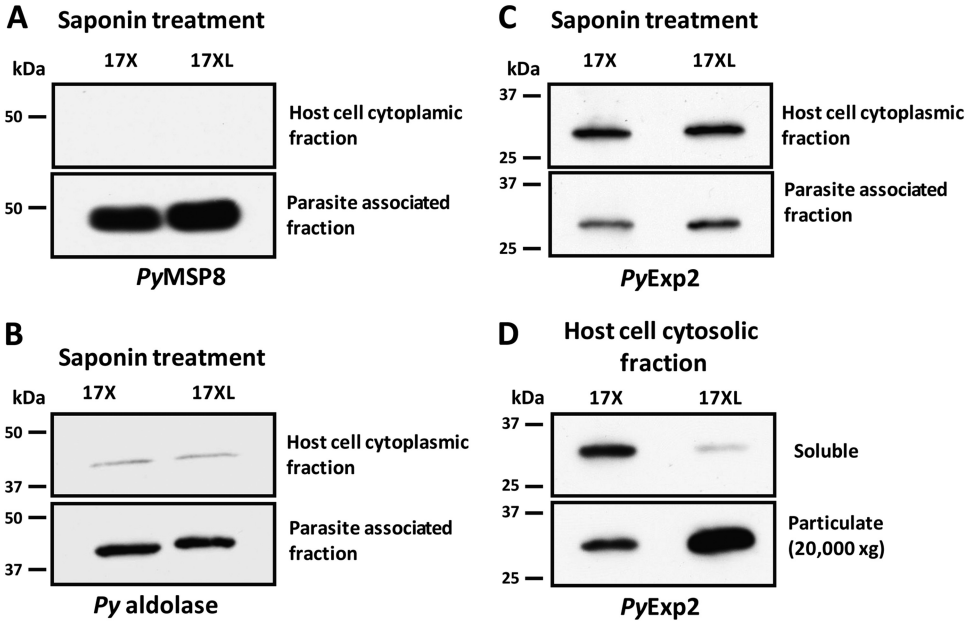

FIG 7 Analysis of host cell cytoplasmic and parasite-associated fractions of *P. yoelii* 17X- and *P. yoelii* 17XL-infected RBCs. Immunoblot analysis of host cell cytoplasmic and parasite-associated fractions obtained by saponin treatment of *P. yoelii* 17X-infected reticulocytes or *P. yoelii* 17XL-infected mature RBCs was performed. Equal volumes of parasite-associated fractions and a 5-fold-larger volume of the host cell cytoplasmic fraction from *P. yoelii* 17X- or *P. yoelii* 17XL-infected RBCs were loaded on the gel. (A to C) The immunoblots were probed with rabbit anti-r*Py*MSP8 antibodies (A), rabbit anti-*P. falciparum* aldolase antibodies (B), or rabbit anti-r*Py*Exp2 sera (C). (D) A soluble fraction and a particulate fraction of the initial host cell cytoplasmic fraction from *P. yoelii* 17X-infected reticulocytes or *P. yoelii* 17XL-infected mature RBCs were obtained by high-speed centrifugation (20,000 × *g*; 45 min). The particulate material was resuspended in SDS-PAGE sample buffer in a volume equal to that of the corresponding soluble supernatant. For immunoblot analysis, equal volumes of soluble and particulate fractions from *P. yoelii* 17X- or *P. yoelii* 17XL-infected RBCs were loaded on the gel and probed with rabbit anti-r*Py*Exp2 sera.

ghei. Focusing the analysis only on RBCs infected with a single parasite, approximately 33% of *P. berghei*-infected reticulocytes and only 21% of *P. berghei*-infected mature RBCs (CD71 negative or low) contained Exp2-positive vesicles. Thus, the formation of Exp2-positive vesicular structures is conserved across two plasmodial species that infect mouse reticulocytes.

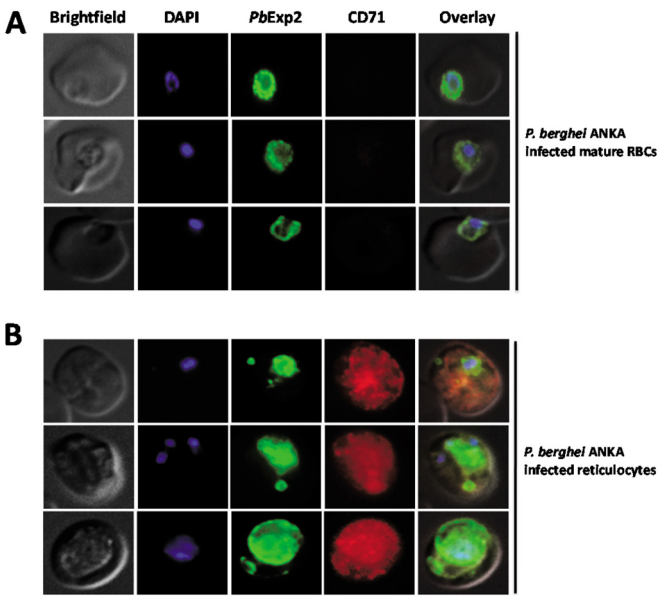

FIG 8 *Pb*Exp2-positive vesicles are preferentially associated with *P. berghei* ANKA-infected reticulocytes. The immunofluorescence images show localization of *Pb*Exp2 (green) in CD71-negative mature RBCs (A) or CD71-positive reticulocytes (B) infected with *P. berghei* ANKA. A suspension-based IFA was performed using mouse anti-r*Py*Exp2 sera and rat anti-mouse CD71 antibody. DAPI was used to stain parasite nuclei (blue).

***P. falciparum*-infected reticulocytes contain Exp2-positive vesicles in the erythrocyte cytoplasm.** It is well established that *P. falciparum* can invade both mature RBCs and reticulocytes (55). However, the growth and development of *P. falciparum* within mature RBCs versus reticulocytes have not been compared in detail due to the difficulty of *in vitro* parasite culture in reticulocytes. Although Exp2 in *P. falciparum* has been mainly characterized as a PVM marker, the above-mentioned *P. yoelii* and *P. berghei* data predict that the localization of *Pf*Exp2 will be altered in parasitized CD71-positive reticulocytes. *P. falciparum* and *P. yoelii* Exp2 proteins share 72% identity and 87% similarity at the amino acid level. As shown in Fig. 9A, anti-r*Py*Exp2 antibodies strongly and specifically recognize the ~32-kDa *Pf*Exp2 in a total antigen lysate of *P. falciparum* FVO blood-stage parasites. Using these anti-r*Py*Exp2 antisera, the localizations of *Pf*Exp2 in mature RBCs and in reticulocytes harboring *P. falciparum* were compared. Human cord blood containing elevated levels of reticulocytes was used for the *in vitro* culture of *P. falciparum* FVO blood-stage parasites (56, 57). With this system, a low number of newly invaded reticulocytes were detected upon staining with Giemsa (Fig. 9B). Immunofluorescence assays were performed using anti-r*Py*Exp2 sera and an anti-human CD71 monoclonal antibody. Consistent with reported data, *Pf*Exp2 was localized exclusively to the intracellular parasite and to the PVM in *P. falciparum*-infected, CD71-negative, mature RBCs (Fig. 9C). As with the rodent parasites, however, *Pf*Exp2-positive vesicles were observed outside the PVM in the host cell cytoplasm when *P. falciparum* was growing in CD71-positive reticulocytes (Fig. 9D). Collectively, these data demonstrate that there are distinct features of the machinery for parasite-

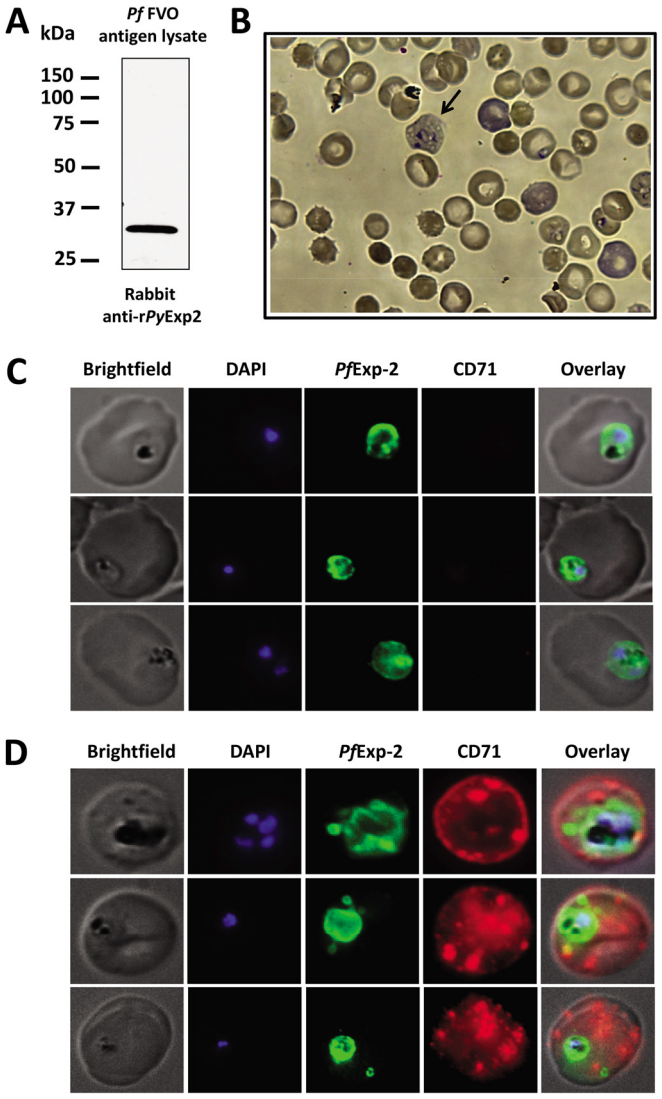

FIG 9 *Pf*Exp2 delineates membranous vesicles in CD71-positive reticulocytes infected with *P. falciparum* strain FVO. (A) Immunoblot analysis of *P. falciparum* FVO parasite lysate (1.6 μg) probed with rabbit anti-r*Py*Exp2 sera. (B) Giemsa-stained image showing *P. falciparum* FVO parasites grown in reticulocyte-enriched human cord blood culture at 16 h postinvasion. The arrow indicates an infected reticulocyte containing a ring-stage parasite. (C and D) Immunofluorescence images showing costaining of *P. falciparum* FVO-infected mature RBCs (C) or recticulocytes (D) for *Pf*Exp-2 (green) and CD71 (red). Rabbit anti-r*Py*Exp2 sera and mouse anti-human CD71 were used for the IFA. DAPI was used to stain parasite nuclei (blue).

directed transport of proteins through the host cell cytoplasm when blood-stage malaria parasites are growing in reticulocytes versus mature RBCs.

DISCUSSION

Extensive studies in *P. falciparum* have led to the identification of distinct parasite-derived structures in mature RBCs, such as MCs (12), the TVN (11), and electron-dense vesicles (18) involved in protein transport across the PVM and the host cytoplasm. Experimental evidence indicates *P. falciparum* parasites utilize PTEX, a large macromolecular complex residing in the PVM, to translocate parasite proteins across the PVM into the red cell cytoplasm (22). In contrast, export pathways that are active in other *Plasmodium* spp. or utilized in different host cell environments are not as well established. This may be partly explained by the limited conservation of known proteins associated with the *P. falciparum* trafficking machinery in other *Plasmodium* species (58). In addition, there has been only limited success in setting up short-term culture systems to support such basic studies of *P. vivax* (57, 59–61). However, it has not been shown if the transport machinery utilized by *P. vivax* is unique or if the reticulocyte cytoplasm influences export. Here, we provide experimental evidence of a novel feature of the protein-trafficking pathway in *Plasmodium*-infected reticulocytes.

Using the rodent *P. yoelii* model, we characterized Exp2, one of the key components of the ATP-dependent PTEX translocon machinery, in *P. falciparum* (22). Based on structural predictions and biochemical data, *Pf*Exp2 is thought to form an oligomeric pore through which parasite proteins are translocated across the PVM (23). Using polyclonal antibodies against r*Py*Exp2, we found that in *P. yoelii* 17X-infected reticulocytes, *Py*Exp2 localizes to the PVM but is also present in the RBC cytoplasm on vesicular structures distinct from the PVM. No staining of such vesicular structures was seen in uninfected reticulocytes. The localization of *Py*Exp2 to the PVM and cytoplasmic vesicles was also verified by using a transgenic parasite line expressing *Py*Exp2 fused to a triple-HA tag (*Py*Exp2-3HA). The vesicles appeared in all blood stages, with a higher frequency during the trophozoite stages. As the intracellular parasites matured, a modest increase in the number of *Py*Exp2-positive cytoplasmic vesicles per iRBC (up to four) was noted. We noted that *Py*Exp2-positive vesicles were typically observed in only a portion of infected reticulocytes. This could in part be due to technical issues related to visualizing a relatively small number of *Py*Exp2-positive vesicles in the correct plane of view. Alternatively, the presence or absence of *Py*Exp2-positive vesicles may further depend on the relative maturity of the host reticulocyte.

We considered the possibility that *Py*Exp2-positive vesicular structures could represent the TVN, which is seen as an extension of the PVM in *P. falciparum* (62). Recent studies also showed pseudopodium- and whorl-like extensions of the PVM in all the blood stages of *P. falciparum* postinvasion (63). As such, we utilized structured-illumination superresolution microscopy to further examine *Py*Exp2 in three dimensions. 3D-SIM analysis clearly identified spherical, *Py*Exp2-positive vesicles not connected to the PVM or to any network of tubular structures in the reticulocyte cytoplasm. The *P. yoelii* vesicles appear significantly larger (>500 nm) than the EDVs (~60 to 100 nm) (17) or J-dots (19) reported in *P. falciparum*. The localization of Exp2 to any distinct structures (i.e., MCs, EDVs, J-dots, etc.) beyond the PVM has not been previously reported. The cytoplasmic *Py*Exp2-positive structures are membranous in nature, as evident from colocalization studies with Bodipy TR ceramide using two-dimensional immunofluorescence and 3D-SIM analysis. Consistently, Bodipy TR ceramide also labeled numerous discrete, punctate structures and tubular structures in the infected reticulocyte cytoplasm that were *Py*Exp2 negative. These may either be parasite and/or host erythrocyte derived (64).

EDVs similar to those involved in the mammalian secretory pathway were reported to be involved in trafficking of *P. falciparum* EMP1 and EMP3 through the iRBC cytoplasm (17). Protein-trafficking pathways in *P. yoelii* are poorly characterized, although

a few *P. yoelii* proteins have been shown to be exported to the host RBC membrane, including those encoded by members of the *yir* multigene family (65), the *P. yoelii* subtelomeric multigene family (*pyst-a*) (47), and tryptophan-rich surface antigens (*Py*pAg-1 and *Py*pAg-3) (45). Members of the *pyst-a* family and an orthologue in *P. berghei* (PBANKA_083680) were specifically shown to be transported to the cytoplasmic side of the erythrocyte membrane (47, 66). In our studies, we found that a *pyst-a* protein (PY04481) and the tryptophan-rich exported protein, *Py*pAg-1 (PY06203), were associated with *Py*Exp2-positive vesicles. These studies also suggested that PY04481 and PY06203 transport can occur independently of *Py*Exp2-positive vesicles and that alternate/redundant pathways are likely.

The PTEX translocon complex in *P. falciparum* (>1,230 kDa) is anchored to the PVM by an Exp2 oligomeric pore (22, 23). Our immunofluorescence and subcellular-fractionation data suggest that a similar, large, membrane-associated complex is present in reticulocytes and mature RBCs infected with *P. yoelii* 17X and *P. yoelii* 17XL parasites, respectively. This complex, still potentially associated with the PVM, can be pelleted from a host cell cytoplasmic fraction released by treatment of iRBCs with saponin. A second soluble species of *Py*Exp2 is detected only in the cytoplasm of *P. yoelii* 17X-infected reticulocytes after high-speed centrifugation. It appears unlikely that this finding can be attributed to a partial disruption of the PVM, as both *P. yoelii* 17X- and *P. yoelii* 17XL-iRBCs were similarly treated with saponin. In the reticulocyte cytoplasm, this soluble form of *Py*Exp2 may be present in a much smaller complex and/or may readily dissociate from *Py*Exp2-positive vesicles. It has yet to be determined how *Py*Exp2-positive vesicles form, but our data indicate that *Py*Exp1 is also associated with these vesicles. The data support the idea that the vesicles pinch or bud off the PVM, trapping proteins (i.e., *Py*pAg-1 and PY04481) present in the parasitophorous vacuolar space in the lumen of the vesicle. In this case, a mechanism to deliver cargo to vesicles in the erythrocyte cytoplasm would not be required.

In addition to the export of proteins to the erythrocyte surface, which may be important for cytoadherence and/or immune evasion, the transport of other proteins to the host plasma membrane is crucial for parasite growth and survival. As earlier studies demonstrated that *exp2* was essential in *P. berghei* (26, 67) and *P. falciparum* (24), it was not a surprise that *pyexp2* was also required for *P. yoelii* viability. While an HA tag could be fused to the 3′ end of the endogenous *pyexp2* gene, the gene was refractory to deletion in both lethal and nonlethal strains of *P. yoelii*. The function and localization of HA-tagged *Py*Exp2 in *P. yoelii*-infected reticulocytes were unaltered. This is also consistent with recent studies in *P. berghei* ANKA showing epitope tagging of *P. berghei* Exp2, as well as other components of PTEX machinery (26). We attempted a conditional knockdown of *Py*Exp2 expression in *P. yoelii* 17X parasites by fusion of an *E. coli* DHFR degradation domain (DDD) to *Py*Exp2 (68). However, fusion of the DDD to the N or C terminus of *Py*Exp2 presumably disrupted function, as we did not obtain viable parasites in the presence of trimethoprim. Combined, our *pyexp2* gene deletion studies confirm the essentiality of Exp2 for *P. yoelii* but cannot distinguish the importance of vesicle-associated *Py*Exp2 versus PVM/PTEX-associated *Py*Exp2 and do not establish whether Exp2-positive vesicles serve a nonredundant, critical function.

P. yoelii is an excellent model to study differences in host-parasite interactions due to the existence of reticulocyte-prone nonlethal *P. yoelii* 17X and the normocyte-prone lethal *P. yoelii* 17XL strains. While *Py*Exp2-positive vesicles were readily formed in CD71-positive, *P. yoelii* 17X-infected reticulocytes, such vesicles were absent in CD71-negative, mature RBCs infected with *P. yoelii* 17XL. We considered that this striking but reproducible finding might be attributed to differences between the *P. yoelii* 17X and *P. yoelii* 17XL strains. However, when growing in CD71-positive reticulocytes induced by phenylhydrazine treatment, *P. yoelii* 17XL readily formed *Py*Exp2-positive vesicles in the host cell cytoplasm. Similarly, with *P. berghei* blood-stage parasites, *Pb*Exp2-positive vesicles were preferentially identified in parasitized CD71-positive reticulocytes. These *Pb*Exp2-positive vesicles appear to be spherical and distinct from the intraerythrocytic *P. berghei*-induced structures (IBIS) (31) or cleft-like structures (32), which are more abundant and tubular. In a study by Curra et al. (33), two members of the *P. berghei* small exported protein (SEP) family were found to be associated with a population of vesicle-like structures in red cell cytoplasm, but it is not known if they form in reticulocytes and/or mature RBCs. Together, these data strongly suggest that in rodent malaria parasites, the protein-trafficking machinery can involve a small number of parasite-derived, Exp2-positive vesicles, distinctly present in parasitized reticulocytes.

Based on previous studies (56, 57), we established a short-term *P. falciparum* invasion assay using reticulocytes enriched from fresh human cord blood. In these cultures, we observed punctate staining of CD71 in reticulocytes (uninfected and infected), which was expected. In culture, reticulocytes mature within 24 to 48 h (48, 64) and lose surface-expressed CD71 (48). Within 48 h following *P. falciparum* merozoite invasion, *Pf*Exp2-positive vesicles formed in CD71-positive reticulocytes but were absent from infected, mature RBCs. Studies to confirm the transport of specific *P. falciparum* proteins by *Pf*Exp2-positive vesicles and the presence of similar pathways in *P. vivax* are needed. However, our data indicate that this novel, reticulocyte-associated feature of the parasite's protein export pathway is conserved in human and rodent malaria parasites.

Compared to circulating mature RBCs, reticulocytes are metabolically active, larger by about 20%, and retain some ribosomes, multivesicular bodies, lysosomes, remnants of mitochondria, Golgi apparatus, and endoplasmic reticulum (64). In a comparative proteome analysis, 587 unique proteins were identified in murine reticulocytes that are absent from mature RBCs. They included several plasma membrane proteins, as well as those involved in intracellular vesicular trafficking (SNAREs, the Rab family, and vesicle-associated membrane protein [VAMP]) (69). While these traffic regulators are thought to be involved in normal reticulocyte maturation (70, 71), it is possible that they also facilitate the budding and/or trafficking of parasite-derived vesicles. In the cytoplasm of *P. yoelii*-infected reticulocytes, we did observe host clathrin-positive structures by immunofluorescence microscopy, which could represent endocytic vesicles, COP-I-containing Golgi apparatus-associated vesicles, and/or free triskelions not associated with any vesicles. However, the *Py*Exp2-positive vesicles were host clathrin negative, indicating that they were parasite derived and likely to be trafficked by exocytic mechanisms. Recent studies have shown that exosome-like vesicles are released from parasitized erythrocytes (72, 73), including from reticulocytes infected with *P. yoelii* (74). Exosomes derived from nonlethal *P. yoelii* 17X-infected reticulocytes were shown to contain several

parasite antigens that modulated host immune responses (74). It will be of interest to determine if Exp2 is involved in the formation, trafficking, or release of these exosomes and if a comparable pathway is active in *P. falciparum*- and *P. vivax*-infected reticulocytes. The studies presented here provide a foundation for such efforts that will further enhance our understanding of malaria parasite development in less-studied reticulocytes and will help to establish the significance of distinct protein-trafficking pathways in specific host cell types.

ACKNOWLEDGMENTS

This work was supported by grant AI1069147 from the National Institute of Allergy and Infectious Diseases of the National Institutes of Health.

We thank Jonathan R. Bowen (Cell Imaging Center, Drexel University) for his technical assistance with 3D-SIM imaging. We thank Stefan Kappe (Seattle Biomedical Research Institute, Seattle, WA) for providing the *Py*Exp1/Hep17-specific MAb.

REFERENCES

1. **Chan M.** 2013. World malaria report 2013. World Health Organization, Geneva, Switzerland.
2. **Pongponratn E, Riganti M, Punpoowong B, Aikawa M.** 1991. Microvascular sequestration of parasitized erythrocytes in human falciparum malaria: a pathological study. Am J Trop Med Hyg **44:**168–175.
3. **Guerra CA, Howes RE, Patil AP, Gething PW, Van Boeckel TP, Temperley WH, Kabaria CW, Tatem AJ, Manh BH, Elyazar IR, Baird JK, Snow RW, Hay SI.** 2010. The international limits and population at risk of Plasmodium vivax transmission in 2009. PLoS Negl Trop Dis **4:**e774. http://dx.doi.org/10.1371/journal.pntd.0000774.
4. **Bessman JD.** 1990. Reticulocytes, p 735–738. *In* Walker HK Hall WD, Hurst JW (ed), Clinical methods: the history, physical, and laboratory examinations, 3rd ed. Butterworths, Boston, MA.
5. **Battle KE, Gething PW, Elyazar IR, Moyes CL, Sinka ME, Howes RE, Guerra CA, Price RN, Baird KJ, Hay SI.** 2012. The global public health significance of Plasmodium vivax. Adv Parasitol **80:**1–111. http://dx.doi.org/10.1016/B978-0-12-397900-1.00001-3.
6. **Deitsch KW, Wellems TE.** 1996. Membrane modifications in erythrocytes parasitized by Plasmodium falciparum. Mol Biochem Parasitol **76:**1–10. http://dx.doi.org/10.1016/0166-6851(95)02575-8.
7. **Rowe JA, Claessens A, Corrigan RA, Arman M.** 2009. Adhesion of Plasmodium falciparum-infected erythrocytes to human cells: molecular mechanisms and therapeutic implications. Expert Rev Mol Med **11:**e16. http://dx.doi.org/10.1017/S1462399409001082.
8. **Desai SA.** 2012. Ion and nutrient uptake by malaria parasite-infected erythrocytes. Cell Microbiol **14:**1003–1009. http://dx.doi.org/10.1111/j.1462-5822.2012.01790.x.
9. **Nguitragool W, Bokhari AA, Pillai AD, Rayavara K, Sharma P, Turpin B, Aravind L, Desai SA.** 2011. Malaria parasite clag3 genes determine channel-mediated nutrient uptake by infected red blood cells. Cell **145:**665–677. http://dx.doi.org/10.1016/j.cell.2011.05.002.
10. **Crabb BS, Cooke BM, Reeder JC, Waller RF, Caruana SR, Davern KM, Wickham ME, Brown GV, Coppel RL, Cowman AF.** 1997. Targeted gene disruption shows that knobs enable malaria-infected red cells to cytoadhere under physiological shear stress. Cell **89:**287–296. http://dx.doi.org/10.1016/S0092-8674(00)80207-X.
11. **Wickert H, Gottler W, Krohne G, Lanzer M.** 2004. Maurer's cleft organization in the cytoplasm of plasmodium falciparum-infected erythrocytes: new insights from three-dimensional reconstruction of serial ultrathin sections. Eur J Cell Biol **83:**567–582. http://dx.doi.org/10.1078/0171-9335-00432.
12. **Spycher C, Rug M, Klonis N, Ferguson DJ, Cowman AF, Beck HP, Tilley L.** 2006. Genesis of and trafficking to the Maurer's clefts of Plasmodium falciparum-infected erythrocytes. Mol Cell Biol **26:**4074–4085. http://dx.doi.org/10.1128/MCB.00095-06.
13. **Kriek N, Tilley L, Horrocks P, Pinches R, Elford BC, Ferguson DJ, Lingelbach K, Newbold CI.** 2003. Characterization of the pathway for transport of the cytoadherence-mediating protein, PfEMP1, to the host cell surface in malaria parasite-infected erythrocytes. Mol Microbiol **50:**1215–1227. http://dx.doi.org/10.1046/j.1365-2958.2003.03784.x.
14. **Newbold C, Warn P, Black G, Berendt A, Craig A, Snow B, Msobo M, Peshu N, Marsh K.** 1997. Receptor-specific adhesion and clinical disease in Plasmodium falciparum. Am J Trop Med Hyg **57:**389–398.
15. **Ockenhouse CF, Tegoshi T, Maeno Y, Benjamin C, Ho M, Kan KE, Thway Y, Win K, Aikawa M, Lobb RR.** 1992. Human vascular endothelial cell adhesion receptors for Plasmodium falciparum-infected erythrocytes: roles for endothelial leukocyte adhesion molecule 1 and vascular cell adhesion molecule 1. J Exp Med **176:**1183–1189. http://dx.doi.org/10.1084/jem.176.4.1183.
16. **Baruch DI, Pasloske BL, Singh HB, Bi X, Ma XC, Feldman M, Taraschi TF, Howard RJ.** 1995. Cloning the P. falciparum gene encoding PfEMP1, a malarial variant antigen and adherence receptor on the surface of parasitized human erythrocytes. Cell **82:**77–87. http://dx.doi.org/10.1016/0092-8674(95)90054-3.
17. **Trelka DP, Schneider TG, Reeder JC, Taraschi TF.** 2000. Evidence for vesicle-mediated trafficking of parasite proteins to the host cell cytosol and erythrocyte surface membrane in Plasmodium falciparum infected erythrocytes. Mol Biochem Parasitol **106:**131–145. http://dx.doi.org/10.1016/S0166-6851(99)00207-8.
18. **Taraschi TF, O'Donnell M, Martinez S, Schneider T, Trelka D, Fowler VM, Tilley L, Moriyama Y.** 2003. Generation of an erythrocyte vesicle transport system by Plasmodium falciparum malaria parasites. Blood **102:**3420–3426. http://dx.doi.org/10.1182/blood-2003-05-1448.
19. **Kulzer S, Rug M, Brinkmann K, Cannon P, Cowman A, Lingelbach K, Blatch GL, Maier AG, Przyborski JM.** 2010. Parasite-encoded Hsp40 proteins define novel mobile structures in the cytosol of the P. falciparum-infected erythrocyte. Cell Microbiol **12:**1398–1420. http://dx.doi.org/10.1111/j.1462-5822.2010.01477.x.
20. **Hiller NL, Bhattacharjee S, van Ooij C, Liolios K, Harrison T, Lopez-Estrano C, Haldar K.** 2004. A host-targeting signal in virulence proteins reveals a secretome in malarial infection. Science **306:**1934–1937. http://dx.doi.org/10.1126/science.1102737.
21. **Marti M, Good RT, Rug M, Knuepfer E, Cowman AF.** 2004. Targeting malaria virulence and remodeling proteins to the host erythrocyte. Science **306:**1930–1933. http://dx.doi.org/10.1126/science.1102452.
22. **de Koning-Ward TF, Gilson PR, Boddey JA, Rug M, Smith BJ, Papenfuss AT, Sanders PR, Lundie RJ, Maier AG, Cowman AF, Crabb BS.** 2009. A newly discovered protein export machine in malaria parasites. Nature **459:**945–949. http://dx.doi.org/10.1038/nature08104.
23. **Bullen HE, Charnaud SC, Kalanon M, Riglar DT, Dekiwadia C, Kangwanrangsan N, Torii M, Tsuboi T, Baum J, Ralph SA, Cowman AF, de Koning-Ward TF, Crabb BS, Gilson PR.** 2012. Biosynthesis, localization, and macromolecular arrangement of the Plasmodium falciparum translocon of exported proteins (PTEX). J Biol Chem **287:**7871–7884. http://dx.doi.org/10.1074/jbc.M111.328591.
24. **Elsworth B, Matthews K, Nie CQ, Kalanon M, Charnaud SC, Sanders PR, Chisholm SA, Counihan NA, Shaw PJ, Pino P, Chan JA, Azevedo MF, Rogerson SJ, Beeson JG, Crabb BS, Gilson PR, de Koning-Ward TF.** 2014. PTEX is an essential nexus for protein export in malaria parasites. Nature **511:**587–591. http://dx.doi.org/10.1038/nature13555.
25. **Beck JR, Muralidharan V, Oksman A, Goldberg DE.** 2014. PTEX component HSP101 mediates export of diverse malaria effectors into host erythrocytes. Nature **511:**592–595. http://dx.doi.org/10.1038/nature13574.
26. **Matthews K, Kalanon M, Chisholm SA, Sturm A, Goodman CD, Dixon MW, Sanders PR, Nebl T, Fraser F, Haase S, McFadden GI, Gilson PR, Crabb BS, de Koning-Ward TF.** 2013. The Plasmodium translocon of exported proteins (PTEX) component thioredoxin-2 is important for maintaining normal blood-stage growth. Mol Microbiol **89:**1167–1186. http://dx.doi.org/10.1111/mmi.12334.
27. **Gehde N, Hinrichs C, Montilla I, Charpian S, Lingelbach K, Przyborski JM.** 2009. Protein unfolding is an essential requirement for transport across the parasitophorous vacuolar membrane of Plasmodium falciparum. Mol Microbiol **71:**613–628. http://dx.doi.org/10.1111/j.1365-2958.2008.06552.x.
28. **Carlton JM, Adams JH, Silva JC, Bidwell SL, Lorenzi H, Caler E, Crabtree J, Angiuoli SV, Merino EF, Amedeo P, Cheng Q, Coulson RM, Crabb BS, Del Portillo HA, Essien K, Feldblyum TV, Fernandez-Becerra C, Gilson PR, Gueye AH, Guo X, Kang'a S, Kooij TW, Korsinczky M, Meyer EV, Nene V, Paulsen I, White O, Ralph SA, Ren Q, Sargeant TJ, Salzberg SL, Stoeckert CJ, Sullivan SA, Yamamoto MM, Hoffman SL, Wortman JR, Gardner MJ, Galinski MR, Barnwell JW, Fraser-Liggett CM.** 2008. Comparative genomics of the neglected human

malaria parasite Plasmodium vivax. Nature **455:**757–763. http://dx.doi.org/10.1038/nature07327.

29. **Aikawa M, Miller LH, Rabbege J.** 1975. Caveola-vesicle complexes in the plasmalemma of erythrocytes infected by Plasmodium vivax and P cynomolgi. Unique structures related to Schuffner's dots. Am J Pathol **79:**285–300.
30. **Barnwell JW, Ingravallo P, Galinski MR, Matsumoto Y, Aikawa M.** 1990. Plasmodium vivax: malarial proteins associated with the membrane-bound caveola-vesicle complexes and cytoplasmic cleft structures of infected erythrocytes. Exp Parasitol **70:**85–99. http://dx.doi.org/10.1016/0014-4894(90)90088-T.
31. **Ingmundson A, Nahar C, Brinkmann V, Lehmann MJ, Matuschewski K.** 2012. The exported Plasmodium berghei protein IBIS1 delineates membranous structures in infected red blood cells. Mol Microbiol **83:**1229–1243. http://dx.doi.org/10.1111/j.1365-2958.2012.08004.x.
32. **Haase S, Hanssen E, Matthews K, Kalanon M, de Koning-Ward TF.** 2013. The exported protein PbCP1 localises to cleft-like structures in the rodent malaria parasite Plasmodium berghei. PLoS One **8:**e61482. http://dx.doi.org/10.1371/journal.pone.0061482.
33. **Curra C, Pace T, Franke-Fayard BM, Picci L, Bertuccini L, Ponzi M.** 2012. Erythrocyte remodeling in Plasmodium berghei infection: the contribution of SEP family members. Traffic **13:**388–399. http://dx.doi.org/10.1111/j.1600-0854.2011.01313.x.
34. **MacKellar DC, Vaughan AM, Aly AS, DeLeon S, Kappe SH.** 2011. A systematic analysis of the early transcribed membrane protein family throughout the life cycle of Plasmodium yoelii. Cell Microbiol **13:**1755–1767. http://dx.doi.org/10.1111/j.1462-5822.2011.01656.x.
35. **Borggraefe I, Yuan J, Telford SR III, Menon S, Hunter R, Shah S, Spielman A, Gelfand JA, Wortis HH, Vannier E.** 2006. Babesia microti primarily invades mature erythrocytes in mice. Infect Immun **74:**3204–3212. http://dx.doi.org/10.1128/IAI.01560-05.
36. **Liu J, Guo X, Mohandas N, Chasis JA, An X.** 2010. Membrane remodeling during reticulocyte maturation. Blood **115:**2021–2027. http://dx.doi.org/10.1182/blood-2009-08-241182.
37. **Shi Q, Cernetich-Ott A, Lynch MM, Burns JM, Jr.** 2006. Expression, localization, and erythrocyte binding activity of Plasmodium yoelii merozoite surface protein-8. Mol Biochem Parasitol **149:**231–241. http://dx.doi.org/10.1016/j.molbiopara.2006.06.002.
38. **Tonkin CJ, van Dooren GG, Spurck TP, Struck NS, Good RT, Handman E, Cowman AF, McFadden GI.** 2004. Localization of organellar proteins in Plasmodium falciparum using a novel set of transfection vectors and a new immunofluorescence fixation method. Mol Biochem Parasitol **137:**13–21. http://dx.doi.org/10.1016/j.molbiopara.2004.05.009.
39. **Fahey JR, Spitalny GL.** 1984. Virulent and nonvirulent forms of Plasmodium yoelii are not restricted to growth within a single erythrocyte type. Infect Immun **44:**151–156.
40. **Behari R, Haldar K.** 1994. Plasmodium falciparum: protein localization along a novel, lipid-rich tubovesicular membrane network in infected erythrocytes. Exp Parasitol **79:**250–259. http://dx.doi.org/10.1006/expr.1994.1088.
41. **Janse CJ, Ramesar J, Waters AP.** 2006. High-efficiency transfection and drug selection of genetically transformed blood stages of the rodent malaria parasite Plasmodium berghei. Nat Protoc **1:**346–356. http://dx.doi.org/10.1038/nprot.2006.53.
42. **Jongco AM, Ting LM, Thathy V, Mota MM, Kim K.** 2006. Improved transfection and new selectable markers for the rodent malaria parasite Plasmodium yoelii. Mol Biochem Parasitol **146:**242–250. http://dx.doi.org/10.1016/j.molbiopara.2006.01.001.
43. **Schermelleh L, Carlton PM, Haase S, Shao L, Winoto L, Kner P, Burke B, Cardoso MC, Agard DA, Gustafsson MG, Leonhardt H, Sedat JW.** 2008. Subdiffraction multicolor imaging of the nuclear periphery with 3D structured illumination microscopy. Science **320:**1332–1336. http://dx.doi.org/10.1126/science.1156947.
44. **Haldar K, Uyetake L, Ghori N, Elmendorf HG, Li WL.** 1991. The accumulation and metabolism of a fluorescent ceramide derivative in Plasmodium falciparum-infected erythrocytes. Mol Biochem Parasitol **49:**143–156. http://dx.doi.org/10.1016/0166-6851(91)90137-U.
45. **Burns JM, Jr, Adeeku EK, Dunn PD.** 1999. Protective immunization with a novel membrane protein of Plasmodium yoelii-infected erythrocytes. Infect Immun **67:**675–680.
46. **Carlton JM, Angiuoli SV, Suh BB, Kooij TW, Pertea M, Silva JC, Ermolaeva MD, Allen JE, Selengut JD, Koo HL, Peterson JD, Pop M, Kosack DS, Shumway MF, Bidwell SL, Shallom SJ, van Aken SE, Riedmuller SB, Feldblyum TV, Cho JK, Quackenbush J, Sedegah M, Shoaibi A, Cummings LM, Florens L, Yates JR, Raine JD, Sinden RE, Harris MA, Cunningham DA, Preiser PR, Bergman LW, Vaidya AB, van Lin LH, Janse CJ, Waters AP, Smith HO, White OR, Salzberg SL, Venter JC, Fraser CM, Hoffman SL, Gardner MJ, Carucci DJ.** 2002. Genome sequence and comparative analysis of the model rodent malaria parasite Plasmodium yoelii yoelii. Nature **419:**512–519. http://dx.doi.org/10.1038/nature01099.
47. **Wunderlich F, Helwig M, Schillinger G, Speth V, Wiser MF.** 1988. Expression of the parasite protein Pc90 in plasma membranes of erythrocytes infected with Plasmodium chabaudi. Eur J Cell Biol **47:**157–164.
48. **Malleret B, Xu F, Mohandas N, Suwanarusk R, Chu C, Leite JA, Low K, Turner C, Sriprawat K, Zhang R, Bertrand O, Colin Y, Costa FT, Ong CN, Ng ML, Lim CT, Nosten F, Renia L, Russell B.** 2013. Significant biochemical, biophysical and metabolic diversity in circulating human cord blood reticulocytes. PLoS One **8:**e76062. http://dx.doi.org/10.1371/journal.pone.0076062.
49. **Bar-Zvi D, Mosley ST, Branton D.** 1988. In vivo phosphorylation of clathrin-coated vesicle proteins from rat reticulocytes. J Biol Chem **263:**4408–4415.
50. **Knapp B, Hundt E, Kupper HA.** 1990. Plasmodium falciparum aldolase: gene structure and localization. Mol Biochem Parasitol **40:**1–12. http://dx.doi.org/10.1016/0166-6851(90)90074-V.
51. **Franke-Fayard B, Janse CJ, Cunha-Rodrigues M, Ramesar J, Buscher P, Que I, Lowik C, Voshol PJ, den Boer MA, van Duinen SG, Febbraio M, Mota MM, Waters AP.** 2005. Murine malaria parasite sequestration: CD36 is the major receptor, but cerebral pathology is unlinked to sequestration. Proc Natl Acad Sci U S A **102:**11468–11473. http://dx.doi.org/10.1073/pnas.0503386102.
52. **Hearn J, Rayment N, Landon DN, Katz DR, de Souza JB.** 2000. Immunopathology of cerebral malaria: morphological evidence of parasite sequestration in murine brain microvasculature. Infect Immun **68:**5364–5376. http://dx.doi.org/10.1128/IAI.68.9.5364-5376.2000.
53. **McNally J, O'Donovan SM, Dalton JP.** 1992. Plasmodium berghei and Plasmodium chabaudi chabaudi: development of simple in vitro erythrocyte invasion assays. Parasitology **105:**355–362. http://dx.doi.org/10.1017/S0031182000074527.
54. **Zuckerman A, Yoeli M.** 1954. Age and sex as factors influencing Plasmodium berghei infections in intact and splenectomized rats. J Infect Dis **94:**225–236. http://dx.doi.org/10.1093/infdis/94.3.225.
55. **Pasvol G, Weatherall DJ, Wilson RJ.** 1980. The increased susceptibility of young red cells to invasion by the malarial parasite Plasmodium falciparum. Br J Haematol **45:**285–295. http://dx.doi.org/10.1111/j.1365-2141.1980.tb07148.x.
56. **Grimberg BT, Scheetz EA, Erickson JJ, Bales JM, David M, Daum-Woods K, King CL, Zimmerman PA.** 2012. Increased reticulocyte count from cord blood samples using hypotonic lysis. Exp Parasitol **132:**304–307. http://dx.doi.org/10.1016/j.exppara.2012.07.006.
57. **Udomsangpetch R, Somsri S, Panichakul T, Chotivanich K, Sirichaisinthop J, Yang Z, Cui L, Sattabongkot J.** 2007. Short-term in vitro culture of field isolates of Plasmodium vivax using umbilical cord blood. Parasitol Int **56:**65–69. http://dx.doi.org/10.1016/j.parint.2006.12.005.
58. **Sargeant TJ, Marti M, Caler E, Carlton JM, Simpson K, Speed TP, Cowman AF.** 2006. Lineage-specific expansion of proteins exported to erythrocytes in malaria parasites. Genome Biol **7:**R12. http://dx.doi.org/10.1186/gb-2006-7-2-r12.
59. **Russell B, Suwanarusk R, Borlon C, Costa FT, Chu CS, Rijken MJ, Sriprawat K, Warter L, Koh EG, Malleret B, Colin Y, Bertrand O, Adams JH, D'Alessandro U, Snounou G, Nosten F, Renia L.** 2011. A reliable ex vivo invasion assay of human reticulocytes by Plasmodium vivax. Blood **118:**e74–e81. http://dx.doi.org/10.1182/blood-2011-04-348748.
60. **Fernandez-Becerra C, Pein O, de Oliveira TR, Yamamoto MM, Cassola AC, Rocha C, Soares IS, de Braganca Pereira CA, del Portillo HA.** 2005. Variant proteins of Plasmodium vivax are not clonally expressed in natural infections. Mol Microbiol **58:**648–658. http://dx.doi.org/10.1111/j.1365-2958.2005.04850.x.
61. **Carvalho BO, Lopes SC, Nogueira PA, Orlandi PP, Bargieri DY, Blanco YC, Mamoni R, Leite JA, Rodrigues MM, Soares IS, Oliveira TR, Wunderlich G, Lacerda MV, del Portillo HA, Araujo MO, Russell B, Suwanarusk R, Snounou G, Renia L, Costa FT.** 2010. On the cytoadhesion of Plasmodium vivax-infected erythrocytes. J Infect Dis **202:**638–647. http://dx.doi.org/10.1086/654815.

62. **Lauer SA, Rathod PK, Ghori N, Haldar K.** 1997. A membrane network for nutrient import in red cells infected with the malaria parasite. Science **276:**1122–1125. http://dx.doi.org/10.1126/science.276.5315.1122.
63. **Riglar DT, Rogers KL, Hanssen E, Turnbull L, Bullen HE, Charnaud SC, Przyborski J, Gilson PR, Whitchurch CB, Crabb BS, Baum J, Cowman AF.** 2013. Spatial association with PTEX complexes defines regions for effector export into Plasmodium falciparum-infected erythrocytes. Nat Commun **4:**1415. http://dx.doi.org/10.1038/ncomms2449.
64. **Gronowicz G, Swift H, Steck TL.** 1984. Maturation of the reticulocyte in vitro. J Cell Sci **71:**177–197.
65. **Cunningham DA, Jarra W, Koernig S, Fonager J, Fernandez-Reyes D, Blythe JE, Waller C, Preiser PR, Langhorne J.** 2005. Host immunity modulates transcriptional changes in a multigene family (yir) of rodent malaria. Mol Microbiol **58:**636–647. http://dx.doi.org/10.1111/j.1365-2958.2005.04840.x.
66. **Fonager J, Pasini EM, Braks JA, Klop O, Ramesar J, Remarque EJ, Vroegrijk IO, van Duinen SG, Thomas AW, Khan SM, Mann M, Kocken CH, Janse CJ, Franke-Fayard BM.** 2012. Reduced CD36-dependent tissue sequestration of Plasmodium-infected erythrocytes is detrimental to malaria parasite growth in vivo. J Exp Med **209:**93–107. http://dx.doi.org/10.1084/jem.20110762.
67. **Matz JM, Matuschewski K, Kooij TW.** 2013. Two putative protein export regulators promote Plasmodium blood stage development in vivo. Mol Biochem Parasitol **191:**44–52. http://dx.doi.org/10.1016/j.molbiopara.2013.09.003.
68. **Iwamoto M, Bjorklund T, Lundberg C, Kirik D, Wandless TJ.** 2010. A general chemical method to regulate protein stability in the mammalian central nervous system. Chem Biol **17:**981–988. http://dx.doi.org/10.1016/j.chembiol.2010.07.009.
69. **Prenni JE, Vidal M, Olver CS.** 2012. Preliminary characterization of the murine membrane reticulocyte proteome. Blood Cells Mol Dis **49:**74–82. http://dx.doi.org/10.1016/j.bcmd.2012.05.002.
70. **Griffiths RE, Kupzig S, Cogan N, Mankelow TJ, Betin VM, Trakarnsanga K, Massey EJ, Lane JD, Parsons SF, Anstee DJ.** 2012. Maturing reticulocytes internalize plasma membrane in glycophorin A-containing vesicles that fuse with autophagosomes before exocytosis. Blood **119:**6296–6306. http://dx.doi.org/10.1182/blood-2011-09-376475.
71. **Johnstone RM, Adam M, Hammond JR, Orr L, Turbide C.** 1987. Vesicle formation during reticulocyte maturation. Association of plasma membrane activities with released vesicles (exosomes). J Biol Chem **262:**9412–9420.
72. **Regev-Rudzki N, Wilson DW, Carvalho TG, Sisquella X, Coleman BM, Rug M, Bursac D, Angrisano F, Gee M, Hill AF, Baum J, Cowman AF.** 2013. Cell-cell communication between malaria-infected red blood cells via exosome-like vesicles. Cell **153:**1120–1133. http://dx.doi.org/10.1016/j.cell.2013.04.029.
73. **Mantel PY, Hoang AN, Goldowitz I, Potashnikova D, Hamza B, Vorobjev I, Ghiran I, Toner M, Irimia D, Ivanov AR, Barteneva N, Marti M.** 2013. Malaria-infected erythrocyte-derived microvesicles mediate cellular communication within the parasite population and with the host immune system. Cell Host Microbe **13:**521–534. http://dx.doi.org/10.1016/j.chom.2013.04.009.
74. **Martin-Jaular L, Nakayasu ES, Ferrer M, Almeida IC, Del Portillo HA.** 2011. Exosomes from Plasmodium yoelii-infected reticulocytes protect mice from lethal infections. PLoS One **6:**e26588. http://dx.doi.org/10.1371/journal.pone.0026588.